



**AALBORG UNIVERSITY**  
DENMARK

**Aalborg Universitet**

## **Mu-Synthesis**

Tøffner-Clausen, S.; Andersen, Palle

*Published in:*

Recent Results in Robust and Adaptive Control, EURACO Workshop Florence 11-14 September 1995

*Publication date:*

1995

*Document Version*

Også kaldet Forlagets PDF

[Link to publication from Aalborg University](#)

*Citation for published version (APA):*

Tøffner-Clausen, S., & Andersen, P. (1995). Mu-Synthesis: A Non-Conservative Methodology for Design of Controllers with Robustness Towards Dynamic and Parametric Uncertainty. I Recent Results in Robust and Adaptive Control, EURACO Workshop Florence 11-14 September 1995 (s. 269-303)

### **General rights**

Copyright and moral rights for the publications made accessible in the public portal are retained by the authors and/or other copyright owners and it is a condition of accessing publications that users recognise and abide by the legal requirements associated with these rights.

- ? Users may download and print one copy of any publication from the public portal for the purpose of private study or research.
- ? You may not further distribute the material or use it for any profit-making activity or commercial gain
- ? You may freely distribute the URL identifying the publication in the public portal ?

### **Take down policy**

If you believe that this document breaches copyright please contact us at [vbn@aub.aau.dk](mailto:vbn@aub.aau.dk) providing details, and we will remove access to the work immediately and investigate your claim.

# $\mu$ -Synthesis – A Non-Conservative Methodology for Design of Controllers with Robustness Towards Dynamic and Parametric Uncertainty

Steen Tøffner-Clausen and Palle Andersen

Aalborg University, Department of Control Engineering, Frederik Bajers Vej 7, DK-9220 Aalborg  
Ø, Denmark.

**Abstract:** This paper provides an introduction to  $\mu$ -synthesis. The main purpose of this work is to illustrate how to utilize the structured singular value  $\mu$  in design of control systems which achieve robust performance in face of both dynamic and parametric uncertainty. The emphasis will be on practical design studies rather than mathematical subtleties. A brief introduction to  $\mu$ -theory will be given. As it turns out, the theory is comprehensibly simple and straight forward. The reason for it not being more well known and recognized comes from the fact that its simpleness is usually hidden in lengthy messy mathematical expressions connected with the problems concerning the computation of  $\mu$ . We will try to avoid this pitfall. Comparisons with standard  $\mathcal{H}_\infty$  control theory will be made. It will be shown how much of the conservativeness inherent in  $\mathcal{H}_\infty$  design may be avoided using  $\mu$  methods. Specifically performance and robustness requirements can be decoupled as opposed to  $\mathcal{H}_\infty$  design. Furthermore parametric uncertainty can be handled without conservativeness. The difference between complex and mixed real and complex  $\mu$  synthesis will be emphasized. The latter unfortunately turns out to be rather difficult. However a new approach to this special case will be suggested. Several case studies will be performed using both complex and mixed  $\mu$ -synthesis.

**Keywords:** Robust control, structured singular values,  $\mu$  analysis,  $\mu$  synthesis, parametric/dynamic uncertainty.

## 1 Introduction

Design of controllers with guaranteed closed loop stability and performance for uncertain plants has been the focus of active research for almost 2 decades now. Most of the research on robust control has focused on  $\mathcal{H}_\infty$  like problems. However it turns out that many practical problems do not readily fit the standard  $\mathcal{H}_\infty$  problem setup since the involved model uncertainty is structured rather than unstructured. This causes any  $\mathcal{H}_\infty$  controller design to be potentially conservative and thus limits the obtainable performance of the closed loop system. In [1] it is furthermore shown that estimated frequency domain model uncertainty ellipses cannot be represented accurately using an unstructured perturbation set.

Fortunately theory exists that non-conservatively handles these problems, namely the *structural singular value* or  $\mu$  theory. In many practical applications  $\mu$  theory is more appropriate for system analysis and controller synthesis.  $\mu$  theory has not been as widely recognized as  $\mathcal{H}_\infty$  theory, probably due to the small amount of literature on  $\mu$  and to the computational difficulties associated with  $\mu$ . Recently however algorithms for computing  $\mu$ <sup>1</sup> have become commercially available through the MATLAB<sup>2</sup>  *$\mu$ -Analysis and Synthesis Toolbox* [2]. Also the literature on  $\mu$  is slowly getting better, see e.g. the excellent introduction to  $\mu$ -analysis by Holohan [3].

---

<sup>1</sup>More accurately: upper and lower bounds on  $\mu$ .

<sup>2</sup>MATLAB is a registered trademark of The MathWorks, Inc.

An approach to controller synthesis using  $\mu$  for complex perturbations, frequently denoted  $D$ - $K$ -iteration, has been known for some time now [4] and controller synthesis for structured complex perturbation sets can be accomplished with the aid of the MATLAB  $\mu$  toolbox.

Unfortunately many practical application problem calls for the use of mixed real and complex perturbation sets. E.g. analysis of plant parameter variations which is an often encountered problem rely on the use of mixed or even purely real perturbation sets. Until recently controller synthesis under mixed perturbation sets was an unsolved problem. A solution to this problem has been given by Young [5, 6]. Unfortunately the synthesis procedure proposed by Young is quite involved. Even though it relies on the same principles it is certainly more mathematically complex than the  $D$ - $K$  iteration procedure used for purely complex perturbation sets.

A different approach for mixed  $\mu$  synthesis has been proposed by Tøffner-Clausen *et al.* [7]. This approach, denoted  $\mu$ - $K$ -iteration is computationally much simpler than the procedure proposed by Young and has been shown to produce quite promising results [1, 7].

The main purpose of this paper is to provide an introduction to robust controller synthesis using the structured singular value  $\mu$ . However, in order to put things into perspective, a survey of robust control design methods using the  $\mathcal{H}_\infty$  approach will be given initially. The role of singular values will be discussed as will some of the commonly used singular value bounded unstructured uncertainty descriptions. The potential conservatism inherent in an unstructured uncertainty assumption will be emphasized. It will be shown how the nominal performance problem and the robust stability problem can be addressed with  $\mathcal{H}_\infty$  methods. However, it turns out that the robust performance problem cannot be nonconservatively formulated in an  $\mathcal{H}_\infty$  framework. Then it will be shown how the structured singular value may be used to overcome the shortcomings of the  $\mathcal{H}_\infty$  approach. Controller design using  $\mu$  will then be presented both for purely complex and for mixed real and complex perturbation structures. Finally two examples will be included to illuminate the different methods.

The remainder of the paper is organized as follows. In Section 2 an introduction to robust control analysis and synthesis is given using singular values ( $\mathcal{H}_\infty$ ). In Section 3 robust stability and performance will be addressed using the structured singular value ( $\mu$ ). Finally in Section 4 two design examples will be given to illustrate the methods and a few general conclusions will be drawn.

## 2 Robust Control Design using Singular Values

Consider the general multivariable feedback scheme shown in Figure 2.1. The plant and controller transfer function matrix are denoted  $G(s)$  and  $K(s)$  respectively. Notice that this is a one-degree-of-freedom control configuration. Often a precompensator is included to improve the transient response of the closed loop system. In that case the feedback controller  $K(s)$  is designed to fulfill mainly the following goals:

- Nominal closed loop stability.
- Nominal performance (disturbance rejection).
- Robust closed loop stability.
- Robust performance.

Robust stability means that the closed loop system is stable under all possible perturbations to the plant  $G(s)$ . Robust performance will be used to indicate that the nominal performance requirements are met under all possible perturbations to the plant  $G(s)$ .

### 2.1 Nominal Stability

The stability of a multivariable feedback control system is determined by the extended or generalized Nyquist stability criterion [8]. .

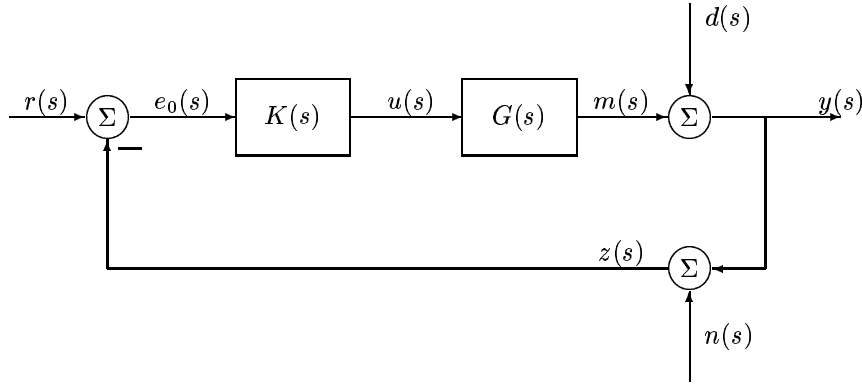


Figure 2.1: General feedback control configuration.

**Theorem 2.1 (Generalized Nyquist Stability Criterion I)** *If the open loop transfer function matrix  $G(s)K(s)$  has  $p$  poles in the right-half  $s$ -plane, then the closed loop system is stable if and only if the map of  $\det(I + G(s)K(s))$ , as  $s$  traverses the Nyquist  $\mathcal{D}$  contour once, encircles the origin  $p$  times anticlockwise assuming no right-half  $s$ -plane zero-pole cancellations have occurred forming the product  $G(s)K(s)$ .*

Remember that the Nyquist  $\mathcal{D}$  contour goes up the imaginary axis from the origin to infinity, then along a semicircular arc in the right half plane until it meets the negative imaginary axis and finally up to the origin. If any poles of  $G(s)K(s)$  are encountered on the imaginary axis the contour is intended so as to include these poles.

An equivalent criterion can be established using *characteristic loci*. If  $\lambda_i(\omega)$  denotes an eigenvalue of  $G(j\omega)K(j\omega)$  the *characteristic loci* is defined as the graphs of  $\lambda_i(\omega)$  for  $1 \leq i \leq n$  where  $n$  is the size of the product  $G(s)K(s)$  as  $j\omega$  encircles the Nyquist  $\mathcal{D}$  contour. Now let  $\Delta \arg$  [rad] denote the change in the argument as  $s$  traverses the  $\mathcal{D}$  contour so that  $\Delta \arg / (2\pi)$  equals the number of origo encirclements. Since the determinant equals the product of the eigenvalues we then have that

$$\begin{aligned} \Delta \arg \{ \det(I + P(s)) \} &= \Delta \arg \left\{ \prod_i \lambda_i(I + P(s)) \right\} = \Delta \arg \left\{ \prod_i (1 + \lambda_i(P(s))) \right\} \\ &= \sum_i \Delta \arg (1 + \lambda_i(P(s))) \quad (2.1) \end{aligned}$$

Since the number of encirclements of  $1 + \lambda_i(P(j\omega))$  around origo equals the number of encirclements of  $\lambda_i(P(j\omega))$  around the Nyquist point  $-1$  we thus have the equivalent generalized Nyquist criterion in Theorem 2.2.

**Theorem 2.2 (Generalized Nyquist Stability Criterion II)** *If the open loop transfer function matrix  $G(s)K(s)$  has  $p$  poles in the right-half  $s$ -plane, then the closed loop system is stable if and only if the characteristic loci of  $G(s)K(s)$  encircle the point  $(-1 + 0j)$   $p$  times anticlockwise assuming no right-half  $s$ -plane zero-pole cancellations have occurred.*

The Generalized Nyquist Stability Criterion will be used in assessing not only nominal stability but also robust stability of an uncertain closed loop system, see Section 2.3.

## 2.2 Nominal performance

From Figure 2.1 it is easily seen that

$$y(s) = T_o(s) (r(s) - n(s)) + S_o(s)d(s) \quad (2.2)$$

$$e_o(s) = S_o(s) (r(s) - d(s) - n(s)) \quad (2.3)$$

$$e(s) = r(s) - y(s) = S_o(s) (r(s) - d(s)) + T_o(s)n(s) \quad (2.4)$$

$$u(s) = M_o(s) (r(s) - n(s) - d(s)) \quad (2.5)$$

where

$$T_o(s) = (I + G(s)K(s))^{-1} G(s)K(s) = G(s)K(s) (I + G(s)K(s))^{-1} \quad (2.6)$$

$$S_o(s) = (I + G(s)K(s))^{-1} \quad (2.7)$$

$$M_o(s) = K(s) (I + G(s)K(s))^{-1} = (I + K(s)G(s))^{-1} K(s) \quad (2.8)$$

are the complementary sensitivity, sensitivity and control sensitivity functions respectively. The subscript  $(\cdot)_o$  emphasizes that the sensitivity functions are all evaluated at the plant output. Since matrix multiplication is not commutative  $G(s)K(s) \neq K(s)G(s)$  in general. It is thus necessary to distinguish between the sensitivity functions evaluated at the plant input and at the plant output, i.e. at the actuators and the sensors respectively. The sensitivity functions at the plant input are given by:

$$T_i(s) = K(s)G(s) (I + K(s)G(s))^{-1} = (I + K(s)G(s))^{-1} K(s)G(s) \quad (2.9)$$

$$S_i(s) = (I + K(s)G(s))^{-1} \quad (2.10)$$

$$M_i(s) = (I + K(s)G(s))^{-1} K(s) \quad (2.11)$$

It is seen that  $M_i(s) = M_o(s) = M(s)$ , so the control sensitivity is independent of the chosen loop breaking point. The relevance of the input sensitivities will become clear shortly.

Now let  $\delta(s) = r(s) - d(s)$  denote the “generic” external disturbance. Then from Equation (2.2)-(2.5) the following observations can be made

- For good disturbance error reduction, that is for  $\delta(s)$  to affect  $e(s)$  to the least extent, (2.4) shows that the sensitivity  $S_o(s)$  should be small.
- For good sensor noise error reduction, that is for  $n(s)$  to affect  $e(s)$  to the least extent, (2.4) shows that the complementary sensitivity  $T_o(s)$  should be small.
- For disturbances  $\delta(s)$  and noise  $n(s)$  to affect the control input  $u(s)$  to the least extent Equation (2.5) shows that the control sensitivity  $M(s)$  should be small.

For scalar systems the size of the (scalar) transfer functions  $S_o(s)$ ,  $T_o(s)$  and  $M(s)$  are naturally measured by the absolute value of the complex valued frequency responses  $|S_o(j\omega)|$ ,  $|T_o(j\omega)|$  and  $|M(j\omega)|$ . However, for multivariable systems the frequency responses  $S_o(j\omega)$ ,  $T_o(j\omega)$  and  $M(j\omega)$  will be complex valued matrices. Thus some scalar measure of the size of a complex valued matrix is needed. Since eigenvalues are used in Theorem 2.2 it is tempting to use the *spectral radius*  $\rho$

$$\rho(A) = \max_i |\lambda_i(A)| \quad (2.12)$$

as measure. It is however a well documented fact, see e.g. [9], that eigenvalues may give poor indication of the “gain” of a transfer function matrix  $G(j\omega)$  if the gain is measured as the 2-norm ratio of the output to the input. Instead it has become standard practice to use *singular values* as gain measure. The singular values of a complex matrix  $A \in \mathbf{C}^{n \times m}$ , denoted  $\sigma_i(A)$ , are the  $k$  largest nonnegative square roots of the eigenvalues of  $A^H A$  where  $k = \min\{n, m\}$  and  $A^H$  denotes the complex conjugate transpose of  $A$ . Thus

$$\sigma_i(A) = \sqrt{\lambda_i(A^H A)} \quad i = 1, 2, \dots, k \quad (2.13)$$

It is usually assumed that the singular values are ordered such that  $\sigma_i \geq \sigma_{i+1}$ . It is then a well known fact that the maximum ( $\bar{\sigma}$ ) and minimum ( $\underline{\sigma}$ ) singular values are also given by

$$\bar{\sigma}(A) = \sigma_1(A) = \max_{u \in \mathbf{C}^m} \frac{|Au|_2}{|u|_2} = \|A\|_2 \quad (2.14)$$

$$\underline{\sigma}(A) = \sigma_k(A) = \min_{u \in \mathbf{C}^m} \frac{|Au|_2}{|u|_2} = \|A^{-1}\|_2^{-1} \quad \text{if } A^{-1} \text{ exists} \quad (2.15)$$

Thus the gain of a complex matrix is limited by the maximum and minimum singular value as the input vector  $u$  varies over all possible directions. Equations (2.14) and (2.15) are one of the main reasons for using singular values to represent the gain of a transfer function matrix. The ratio between the maximum and minimum singular value is denoted the condition number  $\kappa$ :

$$\kappa(A) = \frac{\bar{\sigma}(A)}{\underline{\sigma}(A)} \quad (2.16)$$

Using largest singular value as measure, for good disturbance rejection one would thus require:

$$\bar{\sigma}(S_o(j\omega)) \ll 1 \quad (2.17)$$

Similarly, for good sensor noise rejection one would require:

$$\bar{\sigma}(T_o(j\omega)) \ll 1 \quad (2.18)$$

and for low sensitivity of the input

$$\bar{\sigma}(M(j\omega)) \ll 1 \quad (2.19)$$

However, because  $T_o(j\omega) + S_o(j\omega) = I$  the sensitivity  $S_o(j\omega)$  and the complementary sensitivity  $T_o(j\omega)$  cannot both be small in the same frequency range. Consequently it is demonstrated by (2.17) - (2.18) that optimal tracking or disturbance rejection and optimal sensor noise rejection cannot be obtained *in the same frequency range!* This is a well-known result from classical control. Fortunately the spectra of disturbances  $\delta(s)$  are usually concentrated at low frequencies whereas the spectra of measurement noise  $n(s)$  is concentrated at higher frequencies. Thus one may shape the complementary sensitivity  $T_o(j\omega)$  and the sensitivity  $S_o(j\omega)$  such that  $\bar{\sigma}(S_o(j\omega))$  is small at low frequencies and  $\bar{\sigma}(T_o(j\omega))$  is small at high frequencies. In modern process control systems, sensor noise will frequently not be of practical importance. However, as we shall see in the next section, robustness to unstructured uncertainty places bounds on the sensitivity functions as well.

Often a performance specification for robust control is given as a weighted sensitivity specification:

$$\bar{\sigma}(W_{p2}(j\omega)S_o(j\omega)W_{p1}(j\omega)) \leq 1 \quad \forall \omega \quad (2.20)$$

where  $W_{p1}(s)$  and  $W_{p2}(s)$  denotes the input and output weight respectively, see Figure 2.2. It is assumed that the weights have been scaled such that a unity bound on the RHS makes sense.

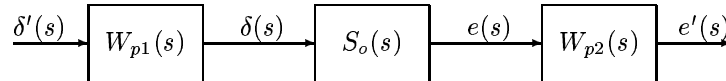


Figure 2.2: Output sensitivity  $S_o(s)$  with input weight  $W_{p1}(s)$  and output weight  $W_{p2}(s)$ .

The *normalized input vector*  $\delta'(s)$  is assumed to belong to the set of normbounded functions

$$\mathcal{D}' = \left\{ \delta' \mid \|\delta'(s)\|_2^2 \leq 1 \right\} \quad (2.21)$$

The input weight  $W_{p1}(s)$  is used to transform the normalized inputs  $\delta'(s)$  to the physical inputs  $\delta(s) = W_{p1}(s)\delta'(s)$ . If e.g. the physical inputs are measured in different units,  $W_{p1}(s)$  is used to normalize  $\delta(s)$  such that  $\delta'(s)$  have equal relative magnitude. The physical inputs are thus assumed to belong to the set

$$\mathcal{D} = \left\{ \delta \mid \|W_{p1}^{-1}(s)\delta(s)\|_2^2 \leq 1 \right\}. \quad (2.22)$$

Treating sets of generic disturbances  $\delta(s)$  is attractive because at the design stage it is rarely possible to predict exactly what type of setpoint changes  $r(s)$  or disturbances  $d(s)$  are going to occur during actual operation. Of course, in principle, the control performance could deteriorate significantly if the assumed disturbances for the design is not exactly equal to the input encountered in practice. Since the spectra of  $\delta$  is usually concentrated at low frequencies,  $W_{p1}(s)$  will generally be large at low frequencies and small at high frequencies. If set-point changes for the different outputs are of primary importance then

$W_{p1}(s) = s^{-1}I$  is a reasonable weight. If, on the other hand, disturbance rejection is more important then  $W_{p1}(s) = G_d(s)$  where  $G_d(s)$  is a disturbance model is more appropriate. See [8] for a thorough analysis of input weights.

The output weight  $W_{p2}(s)$  is used to trade off the relative importance of the individual errors in  $e(s)$  and to weigh the frequency range of primary interest.

The nominal performance objective is thus, given weighting functions  $W_{p1}(s)$  and  $W_{p2}(s)$ , to design a stabilizing controller  $K(s)$  such that the cost function

$$\mathcal{J}_{np} = \|W_{p2}(s)S_o(s)W_{p1}(s)\|_{\infty} \quad (2.23)$$

is minimized. Thus

$$K(s) = \inf_{K(s) \in \mathcal{K}_S} \|W_{p2}(s)S_o(s)W_{p1}(s)\|_{\infty} \quad (2.24)$$

where  $\mathcal{K}_S$  denotes the set of all stabilizing controllers and  $\inf(\cdot)$  denotes the infimum. If a controller can achieve  $\|W_{p2}(s)S_o(s)W_{p1}(s)\|_{\infty} < 1$ , we say that the closed loop system has *nominal performance*. A very convenient way of formulating the nominal performance problem is by use of the *2x2 Block Problem Formulation*. In Figure 2.3 it is shown how the weights  $W_{p1}(s)$  and  $W_{p2}(s)$  may be include into the closed loop system in Figure 2.1. The augmented closed loop system may then be represented as a  $2 \times 2$  block problem. The *generalized plant*  $N(s)$  contains the nominal plant  $G(s)$  as well as weighting functions to reflect nominal performance objectives. The reference  $r(s)$  may be included in  $d'(s)$  or otherwise the response to set-point changes may be formed separately by the use of prefilters.

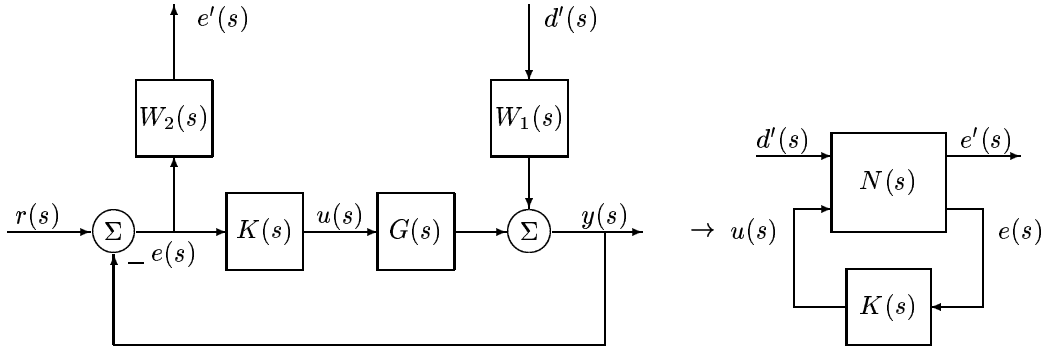


Figure 2.3: *Nominal performance problem. Augmented closed loop system and corresponding  $2 \times 2$  block problem.*

The transfer function from  $d'(s)$  to  $e'(s)$  is given by the *linear fractional transformation* (LFT):

$$e'(s) = F_l(N(s), K(s))d'(s) = (N_{11}(s) + N_{12}(s)K(s)(I - N_{22}(s)K(s))^{-1}N_{21}(s)) d'(s) \quad (2.25)$$

$$= W_{p2}(s)S_o(s)W_{p1}(s)d'(s) \quad (2.26)$$

Now the optimal nominal performance problem is one of finding a controller such that:

$$K(s) = \inf_{K(s) \in \mathcal{K}_S} \|F_l(N(s), K(s))\|_{\infty}. \quad (2.27)$$

The problem (2.27) is a standard  $\mathcal{H}_{\infty}$  problem which can be solved with well-known techniques, see Section 2.5.

## 2.3 Robust Stability

At this point we will consider only unstructured complex perturbations like e.g.

- Additive uncertainty:  $\tilde{G}(s) = G(s) + \tilde{\Delta}(s)$ .

- Input multiplicative uncertainty:  $\tilde{G}(s) = G(s)(I + \tilde{\Delta}(s))$ .
- Output multiplicative uncertainty:  $\tilde{G}(s) = (I + \tilde{\Delta}(s))G(s)$ .
- Inverse input multiplicative uncertainty:  $\tilde{G}(s) = G(s)(I + \tilde{\Delta}(s))^{-1}$ .
- Inverse output multiplicative uncertainty:  $\tilde{G}(s) = (I + \tilde{\Delta}(s))^{-1}G(s)$ .

where  $\tilde{\Delta}(s)$  obeys:

$$\bar{\sigma}(\tilde{\Delta}(j\omega)) \leq \ell(\omega), \quad \forall \omega \geq 0 \quad (2.28)$$

The perturbation  $\tilde{\Delta}(j\omega)$  is thus a full complex matrix bounded only in magnitude. Usually two diagonal weighting matrices  $W_{u1}(s)$  and  $W_{u2}(s)$  are introduced such that

$$\tilde{\Delta}(s) = W_{u2}(s)\Delta(s)W_{u1}(s) \quad (2.29)$$

and  $\bar{\sigma}(\Delta)(j\omega) \leq 1, \forall \omega$ . If any structural information of  $\tilde{\Delta}(s)$  is available, e.g. of the relative magnitude of the individual elements,  $W_{u1}(s)$  and  $W_{u2}(s)$  should be chosen in order to reflect this as adequately or non-conservatively as possible, e.g. such that all elements in  $\Delta(s)$  are of the same magnitude, see Example 2.1. However, this is not naturally performed using unstructured perturbations. If structural information of  $\tilde{\Delta}(s)$  is available it is much more natural to use the structured singular value approach as outlined in Section 3.

**Example 2.1 (Structured Uncertainty with Full Perturbation Block)** *Assume that an uncertainty analysis has resulted in an additive uncertainty model  $\tilde{G}(s) = G(s) + \tilde{\Delta}(s)$  with*

$$\tilde{\Delta}(s) = \frac{K}{1 + \tau s} \begin{bmatrix} 10\delta_{11} & \delta_{12} \\ 0.1\delta_{21} & \delta_{22} \end{bmatrix} \quad (2.30)$$

where  $\delta_{ii} \in \mathbf{C}$ ,  $|\delta_{ii}| \leq 1$ . Notice that this corresponds to each element of the plant transfer function being confined to a disc in the Nyquist plane at each frequency  $\omega$ . It is thus a structured description of the uncertainty. Since  $\bar{\sigma}([10 \ 1; 0.1 \ 1]) = 10.05$  we have that

$$\bar{\sigma}(\tilde{\Delta}(j\omega)) \leq \frac{10.05K}{1 + \tau j\omega} \quad (2.31)$$

We now must introduce weighting matrices such that the scaled uncertainty block  $\Delta(s)$  satisfy  $\bar{\sigma}(\Delta(s)) \leq 1$ . A simple choice would be

$$W_{u1}(s) = \frac{10.05K}{1 + \tau s} \cdot I_2, \quad W_{u2}(s) = I_2 \quad (2.32)$$

Then the corresponding  $\Delta(s)$  would be

$$\Delta(s) = \frac{1}{10.05} \begin{bmatrix} 10\delta_{11} & \delta_{12} \\ 0.1\delta_{21} & \delta_{22} \end{bmatrix} \approx \begin{bmatrix} \delta_{11} & 0.1\delta_{12} \\ 0.01\delta_{21} & 0.1\delta_{22} \end{bmatrix}. \quad (2.33)$$

Assuming an unstructured uncertainty description we will approximate (2.33) with a full complex block. This will, however, be a rather conservative approximation since the size of the different elements in  $\Delta(s)$  are different up till a factor 100. If we instead choose

$$W_{u1}(s) = I_2, \quad W_{u2}(s) = \frac{1.1K}{1 + \tau s} \begin{bmatrix} 10 & 0 \\ 0 & 1 \end{bmatrix} \quad (2.34)$$

Then the corresponding  $\Delta(s)$  would be

$$\Delta(s) = \frac{1}{1.1} \begin{bmatrix} \delta_{11} & 0.1\delta_{12} \\ 0.1\delta_{21} & \delta_{22} \end{bmatrix} \quad (2.35)$$

and we have reduced the relative magnitude to 10. Consequently a full complex block approximation will be less conservative.

If no information of the structure of the perturbation  $\tilde{\Delta}(s)$  is available,  $W_{u1}(s) = I$  and  $W_{u2}(s) = w_u(s) \cdot I$  with  $|w_u(j\omega)| = \ell(\omega)$  or visa-versa would be a natural choice.



### 2.3.1 The Small Gain Theorem

Now the celebrated *Small Gain Theorem*, see e.g. [10], will be introduced and applied in connection with the above uncertainty structures. Consider the closed loop system in Figure 2.1 and let  $P(s) = G(s)K(s)$  be a square transfer function matrix.

**Theorem 2.3 (Small Gain Theorem)** *Assume that  $P(s)$  is stable. Then the closed loop system is stable if the spectral radius  $\rho(P(j\omega)) < 1, \forall \omega$ .*

**Proof of Theorem 2.3 (By contradiction)** Assume that the spectral radius  $\rho(P(j\omega)) < 1, \forall \omega$  and that the closed loop system is unstable. Applying Theorem 2.1 instability implies that the map of  $\det(I + P(s))$  encircles the origin as  $s$  traverses the Nyquist  $\mathcal{D}$  contour. Because the Nyquist contour is closed so is the map of  $\det(I + P(s))$ . Then there exists an  $\epsilon \in [0, 1]$  and a frequency  $\omega^*$  such that

$$\det(I + \epsilon P(j\omega^*)) = 0 \quad \text{i.e. the map goes through the origin} \quad (2.36)$$

$$\Leftrightarrow \prod_i \lambda_i(I + \epsilon P(j\omega^*)) = 0 \quad (2.37)$$

$$\Leftrightarrow 1 + \epsilon \lambda_i(P(j\omega^*)) = 0 \quad \text{for some } i \quad (2.38)$$

$$\Leftrightarrow \lambda_i(P(j\omega^*)) = -\frac{1}{\epsilon} \quad \text{for some } i \quad (2.39)$$

$$\Rightarrow |\lambda_i(P(j\omega^*))| \geq 1 \quad \text{for some } i \quad (2.40)$$

which is a contradiction since we assumed that  $\rho(P(j\omega)) < 1, \forall \omega$ . □

Theorem 2.3 states that for an open-loop stable system, a sufficient condition for closed loop stability is to keep the loop “gain” measured by  $\rho(P(j\omega))$  less than unity. Fortunately this is only a sufficient condition for stability. Otherwise the usual performance requirement of high controller gain for low frequencies could not be achieved. Theorem 2.3 thus provides only a sufficient, that is a potentially conservative, condition for stability.

The Small Gain Theorem will now be used to assess the closed loop stability under unstructured norm-bounded perturbations like (2.28). This application is classic in  $\mathcal{H}_\infty$  control theory. A famous and often quoted paper on this is [11]. Let us e.g. assume an additive perturbation:

$$\tilde{G}(s) = G(s) + W_{u2}(s)\Delta(s)W_{u1}(s) \quad (2.41)$$

where  $\bar{\sigma}(\Delta(j\omega)) \leq 1$ . This can be represented in block-diagram form as in Figure 2.4. Let  $P(s)$  denote the transfer matrix “seen” by  $\Delta$ , see also Figure 2.4. It is easily seen that  $P(s) = W_{u1}(s)K(s)(I + G(s)K(s))^{-1}W_{u2}(s) = W_{u1}(s)M(s)W_{u2}(s)$ . We then have the following theorem.

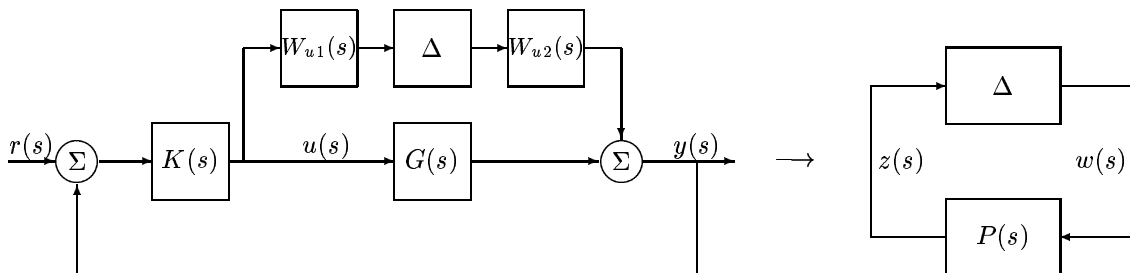


Figure 2.4: Closed loop system with additive perturbation.  $P(s) = W_{u1}(s)K(s)(I + G(s)K(s))^{-1}W_{u2}(s)$  denotes the transfer function “seen” by the perturbation  $\Delta$ .

**Theorem 2.4 (Robust Stability)** *Assume that the interconnection  $P(s)$  is stable and that the perturbation  $\Delta(s)$  is of such a form that the perturbed closed loop system is stable if and only if the map of  $\det(I - P(s)\Delta(s))$  as  $s$  traverses the  $\mathcal{D}$  contour does not encircle the origin. Then the closed loop system*

in Figure 2.4 is stable for all perturbations  $\Delta(s)$  with  $\bar{\sigma}(\Delta(j\omega)) \leq 1$  if and only if one of the following three equivalent conditions are satisfied:

$$\det(I - P(j\omega)\Delta(j\omega)) \neq 0 \quad \forall \omega, \forall \Delta(j\omega) \ni \bar{\sigma}(\Delta(j\omega)) \leq 1 \quad (2.42)$$

$$\Leftrightarrow \rho(P(j\omega)\Delta(j\omega)) < 1 \quad \forall \omega, \forall \Delta(j\omega) \ni \bar{\sigma}(\Delta(j\omega)) \leq 1 \quad (2.43)$$

$$\Leftrightarrow \bar{\sigma}(P(j\omega)) < 1 \quad \forall \omega \quad (2.44)$$

$$\Leftrightarrow \|P(s)\|_\infty < 1 \quad (2.45)$$

**Proof of Theorem 2.4** Assume that there exist a perturbation  $\Delta^*(s)$  such that  $\bar{\sigma}(\Delta^*(j\omega)) \leq 1$  and that the closed loop system is unstable. Then the map of  $\det(I - P(s)\Delta(s))$  encircles the origin as  $s$  traverses the Nyquist  $\mathcal{D}$  contour. Because the Nyquist contour is closed so is the map of  $\det(I - P(s)\Delta(s))$ . Consequently there exists an  $\epsilon \in [0, 1]$  and a frequency  $\omega^*$  such that

$$\det(I - P(j\omega^*)\epsilon\Delta^*(j\omega^*)) = 0. \quad (2.46)$$

Since

$$\bar{\sigma}(\epsilon\Delta^*(j\omega^*)) = \epsilon\bar{\sigma}(\Delta^*(j\omega^*)) \leq 1 \quad (2.47)$$

$\epsilon\Delta^*(s)$  is just another perturbation from the set of possible perturbations. Thus the closed loop system is stable if and only if (2.42) is satisfied. The sufficiency of (2.43) follows directly from Theorem 2.3. Since

$$\rho(P(j\omega)\Delta(j\omega)) \leq \bar{\sigma}(P(j\omega)\Delta(j\omega)) \leq \bar{\sigma}(P(j\omega))\bar{\sigma}(\Delta(j\omega)) \leq \bar{\sigma}(P(j\omega)) \leq \|P(s)\|_\infty \quad (2.48)$$

both (2.44) and (2.45) are sufficient conditions for closed loop stability.

To prove necessity of (2.43) assume that is a  $\Delta^*(s)$  for which  $\bar{\sigma}(\Delta^*(j\omega)) \leq 1$  and a frequency  $\omega^*$  such that  $\rho(P(j\omega^*)\Delta^*(j\omega^*)) = 1$ . Then

$$|\lambda_i(P(j\omega^*)\Delta^*(j\omega^*))| = 1 \quad \text{for some } i \quad (2.49)$$

$$\Leftrightarrow \lambda_i(P(j\omega^*)\Delta^*(j\omega^*)) = e^{j\theta} \quad \text{for some } i \quad (2.50)$$

$$\Leftrightarrow \lambda_i(P(j\omega^*)e^{-j\theta}\Delta^*(j\omega^*)) = +1 \quad \text{for some } i \quad (2.51)$$

$$\Leftrightarrow \lambda_i(P(j\omega^*)\tilde{\Delta}^*(j\omega^*)) = +1 \quad \text{for some } i \quad (2.52)$$

where  $\tilde{\Delta}^*(s)$  is just another perturbation from the set and  $\rho(P(j\omega^*)\tilde{\Delta}^*(j\omega^*)) = 1$ . Therefore

$$\det(I - P(j\omega^*)\tilde{\Delta}^*(j\omega^*)) = 0 \quad (2.53)$$

and the necessity of (2.43) has been shown.

To prove necessity of (2.44) we will show that there exists a perturbation  $\Delta^*(s)$  for which  $\bar{\sigma}(\Delta^*(j\omega)) \leq 1$  such that  $\det(I - P(j\omega^*)\Delta^*(j\omega^*)) = 0$  if  $\bar{\sigma}(P(j\omega^*)) = 1$ . To do so, let  $D = \text{diag}\{1, 0, \dots, 0\}$  and perform a singular value decomposition of  $P(j\omega^*)$ :

$$P(j\omega^*) = U\Sigma V^H \quad (2.54)$$

where  $U$  and  $V$  are unitary matrices. Let  $\Delta^*(j\omega^*) = VDU^H$ . Since  $U$  and  $V$  are unitary  $\bar{\sigma}(\Delta^*) = 1$ . We then have that

$$\begin{aligned} \det(I - P(j\omega^*)\Delta^*(j\omega^*)) &= \det(I - U\Sigma V^H V D U^H) = \det(I - U\Sigma D U^H) = \\ &= \det(U(I - \Sigma D)U^H) = \det(U) \det(I - \Sigma D) \det(U^H) = \det(I - \Sigma D) = 0 \end{aligned} \quad (2.55)$$

since the first row and column in  $I - \Sigma D$  are zero. In fact, there exists an infinite number of perturbations for which (2.55) is fulfilled since we may choose  $D = \text{diag}\{1, \sigma_2, \dots, \sigma_k\}$  where  $\sigma_i \leq 1$  for  $i = 2, \dots, k$ .  $\square$

The above proof is due to Lethomaki [12]. Theorem 2.4 states that if  $\|P(s)\|_\infty < 1$ , there is no perturbation  $\Delta(s)$  ( $\bar{\sigma}(\Delta(j\omega)) \leq 1$ ) which makes  $\det(I - P(s)\Delta(s))$  encircle the origin as  $s$  traverses the Nyquist  $\mathcal{D}$  contour. Notice that we *assumed* that the absence of encirclements is necessary and sufficient to maintain

stability. This is the case, for example, when all perturbations  $\Delta(s)$  are stable or when  $\tilde{G}(s)$  and  $G(s)$  has the same number of unstable (right half plane) poles. One of these assumptions are standard in robust control.

Notice that the  $\infty$ -norm constraint (2.45) in Theorem 2.4 is *not* conservative since we have bounded the uncertainty in terms of the spectral norm (maximum singular value). Thus if  $\|P(s)\|_\infty \geq 1$  there exists a perturbation  $\Delta^*(s)$  for which  $\bar{\sigma}(\Delta^*(j\omega)) \leq 1$  that will destabilize the closed loop system. If the uncertainty is tightly represented by  $\Delta(s)$ , then the singular value bound on  $P(j\omega)$  is thus a tight robustness bound.

Now let us return to the additively perturbed closed loop system in Figure 2.4. From Theorem 2.4, robust stability of the closed loop system is thus obtained if and only if

$$\bar{\sigma}(P(j\omega)) < 1 \quad \forall \omega \quad (2.56)$$

$$\Leftrightarrow \bar{\sigma} \left( W_{u1}(j\omega)K(j\omega) (I + G(j\omega)K(j\omega))^{-1} W_{u2}(j\omega) \right) < 1 \quad \forall \omega \quad (2.57)$$

$$\Leftrightarrow \bar{\sigma} (W_{u1}(j\omega)M(j\omega)W_u(j\omega)) < 1 \quad \forall \omega \quad (2.58)$$

As for additive uncertainty, we may compute singular value bounds that ensure robust stability under other perturbation models. In Table 2.1 results are given for the uncertainty structures introduced previously.

Perturbation	Stability demand	Norm bound
Additive uncertainty	Control sensitivity small	$\ W_{u1}(s)M(s)W_{u2}(s)\ _\infty < 1$
Input multiplicative uncertainty	Comp. sensitivity (input) small	$\ W_{u1}(s)T_i(s)W_{u2}(s)\ _\infty < 1$
Output multiplicative uncertainty	Comp. sensitivity (output) small	$\ W_{u1}(s)T_o(s)W_{u2}(s)\ _\infty < 1$
Inverse input mult. uncertainty	Input sensitivity small	$\ W_{u1}(s)S_i(s)W_{u2}(s)\ _\infty < 1$
Inverse output mult. uncertainty	Output sensitivity small	$\ W_{u1}(s)S_o(s)W_{u2}(s)\ _\infty < 1$

Table 2.1: *Different uncertainty descriptions and their influence on the sensitivity functions.*

The robust stability objective is thus, given e.g. an additive uncertainty specification  $W_{u2}(s)\Delta(s)W_{u1}(s)$ , to design a nominally stabilizing controller  $K(s)$  such that the cost function

$$\mathcal{J}_u = \|W_{u1}(s)M(s)W_{u2}(s)\|_\infty \quad (2.59)$$

is minimized. Thus

$$K(s) = \inf_{K(s) \in \mathcal{K}_S} \|W_{u1}(s)M(s)W_{u2}(s)\|_\infty \quad (2.60)$$

where  $\mathcal{K}_S$  denotes the set of all nominally stabilizing controllers. If a controller can achieve  $\mathcal{J}_u < 1$ , we say that the closed loop system is *robustly stable*. Notice then how the structure of the robust stability problem (2.60) equals the structure of the nominal performance problem (2.24). Consequently the robust stability problem may be formulated as a  $2 \times 2$  block problem as well. Given an additive uncertainty specification, a  $2 \times 2$  block problem formulation may be derived, see Figure 2.5. Compare also with Figure 2.4.

The transfer function from  $w(s)$  to  $z(s)$  is given by the LFT

$$\begin{aligned} z(s) &= F_l(N(s), K(s))w(s) = W_{u1}(s)K(s) (I + G(s)K(s))^{-1} W_{u2}(s)w(s) \\ &= W_{u1}(s)M(s)W_{u2}(s)w(s). \end{aligned} \quad (2.61)$$

The optimal robust stability problem is thus one of finding the controller given by

$$K(s) = \inf_{K(s) \in \mathcal{K}} \|F_l(N(s), K(s))\|_\infty. \quad (2.62)$$

Like the nominal performance problem, the robust stability problem (2.62) is a standard  $\mathcal{H}_\infty$  problem with a known solution.

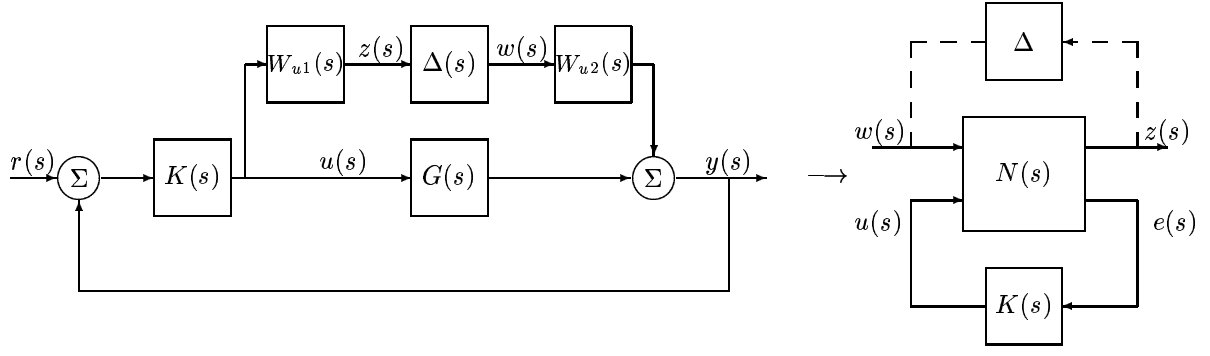


Figure 2.5: Uncertain closed loop system and corresponding  $2 \times 2$  block problem.

## 2.4 Robust Performance

The robust performance objective is of course derived from (2.23) with nominal sensitivity  $S_o(s)$  replaced by perturbed sensitivity  $\tilde{S}_o(s)$ :

$$\mathcal{J}_{rp} = \left\| W_{p2}(s) \tilde{S}_o(s) W_{p1}(s) \right\|_{\infty} \quad (2.63)$$

where  $\tilde{S}_o(s)$  denotes the perturbed sensitivity function. Let us once more illustrate with an additive uncertainty model. The robust performance problem can then be formulated as in Figure 2.6.

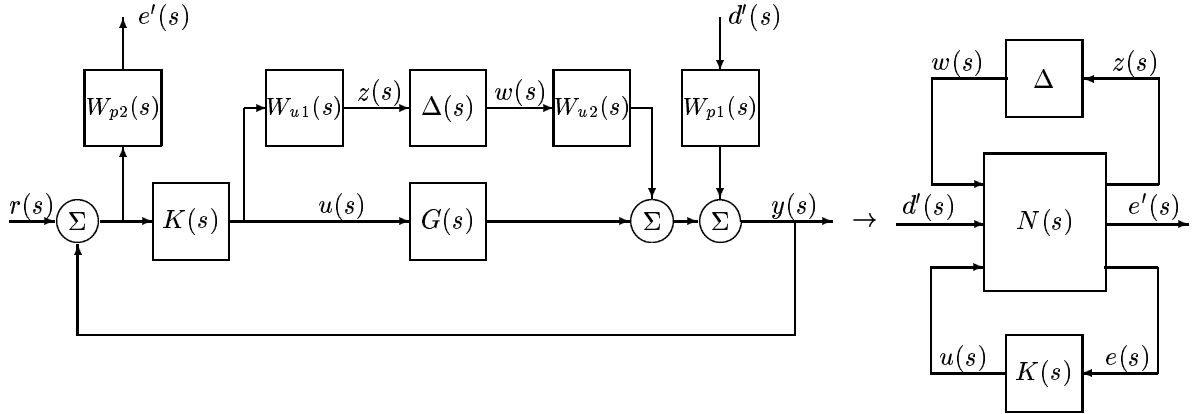


Figure 2.6: Robust performance problem with additive uncertainty.

Let  $P(s) = F_l(N(s), K(s))$ . Then the transfer function from  $d'(s)$  to  $e'(s)$  is given by the LFT

$$e'(s) = F_u(P(s), \Delta(s)) d'(s) = \left[ P_{22}(s) + P_{21}(s) \Delta(s) (I - P_{11}(s) \Delta(s))^{-1} P_{12}(s) \right] d'(s) \quad (2.64)$$

$$= W_{p2}(s) (I + G(s)K(s) + G(s)W_{u2}(s)\Delta(s)W_{u1}(s))^{-1} W_{p1}(s) \quad (2.65)$$

$$= W_{p2}(s) \tilde{S}_o(j\omega) W_{p1}(s) \quad (2.66)$$

The optimal robust performance problem can then be formulated

$$K(s) = \inf_{K(s) \in \mathcal{K}} \|F_u(F_l(N(s), K(s)), \Delta(s))\|_{\infty} \quad (2.67)$$

If

$$\|F_u(F_l(N(s), K(s)), \Delta(s))\|_{\infty} = \|F_u(P(s), \Delta(s))\|_{\infty} < 1 \quad (2.68)$$

we say that closed loop system has *robust performance*. Notice that the robust performance condition (2.68) is similar to the robust stability condition (2.45) in Theorem 2.4. Hence we conclude: *the system  $F_u(P(s), \Delta(s))$  satisfies the robust performance condition (2.68) if and only if it is robustly*

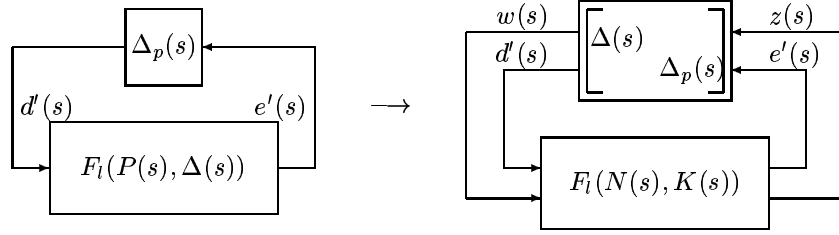


Figure 2.7: Block diagram structure for robust performance check. The perturbation structure is augmented with a full complex performance block  $\Delta_p(s)$ .

stable for a norm bounded matrix perturbation  $\Delta_p(s)$  with  $\bar{\sigma}(\Delta_p(j\omega)) \leq 1$ . Thus by augmenting the perturbation structure with a full complex performance block  $\Delta_p(s)$  the robust performance condition can be equivalenced with a robust stability condition, see also Figure 2.7.

Let  $\tilde{\Delta}(s) = \text{diag}\{\Delta(s), \Delta_p(s)\}$  denote the augmented perturbation matrix. We then have the following theorem.

**Theorem 2.5 (Robust Performance)** Assume that the interconnection  $P(s) = F_l(N(s), K(s))$  is stable and that the perturbation  $\tilde{\Delta}(s)$  is of such a form that the perturbed closed loop system in Figure 2.7 is stable if and only if the map of  $\det(I - P(s)\tilde{\Delta}(s))$  as  $s$  traverses the  $\mathcal{D}$  contour does not encircle the origin. Then the system  $F_u(P(s), \tilde{\Delta}(s))$  will satisfy the robust performance criterion (2.68) if and only if  $P(s)$  is stable for all perturbations  $\tilde{\Delta}(s)$  with  $\bar{\sigma}(\tilde{\Delta}(j\omega)) \leq 1$ :

$$\det(I - P(j\omega)\tilde{\Delta}(j\omega)) \neq 0 \quad \forall \omega, \forall \tilde{\Delta}(j\omega) \ni \bar{\sigma}(\tilde{\Delta}(j\omega)) \leq 1 \quad (2.69)$$

$$\Leftrightarrow \rho(P(j\omega)\tilde{\Delta}(j\omega)) < 1 \quad \forall \omega, \forall \tilde{\Delta}(j\omega) \ni \bar{\sigma}(\tilde{\Delta}(j\omega)) \leq 1 \quad (2.70)$$

$$\Leftarrow \|P(s)\|_\infty < 1 \quad (2.71)$$

**Proof of Theorem 2.5** Follows from Theorem 2.4. Since the structure on  $\tilde{\Delta}(s)$  is restricted, (2.71) is a sufficient condition only.  $\square$

Clearly robust performance implies both nominal performance and robust stability. Thus a necessary condition for robust performance in connection with additive uncertainty is:

$$\mathcal{J}_{np} = \|W_{p2}(s)S_o(s)W_{p1}(s)\|_\infty < 1 \quad (2.72)$$

$$\mathcal{J}_u = \|W_{u1}(s)M(s)W_{u2}(s)\|_\infty < 1 \quad (2.73)$$

A sufficient conditions for robust performance is that the transfer function  $F_l(N(s), K(s))$  from  $[w(s); d'(s)]$  to  $[z(s); e'(s)]$  has  $\infty$ -norm less than one. We may thus formulated an  $\mathcal{H}_\infty$  problem:

$$K(s) = \inf_{K(s) \in \mathcal{K}} \|F_l(N(s), K(s))\|_\infty \quad (2.74)$$

with a known solution. If

$$\|F_l(N(s), K(s))\|_\infty < 1 \quad (2.75)$$

the closed loop system will have robust performance. However, since (2.71) is a sufficient condition only it may be arbitrarily conservative. The next two examples will shed some light on this issue.

**Example 2.2 (Robust Performance Problem I)** Assume that a performance specification on the output sensitivity function  $S_o(s)$  of the form (2.20) is given. Also an additive robust stability specification on the control sensitivity function  $M(s)$  of the form (2.58) is assumed. The problem considered is thus the one illustrated in Figure 2.6. The closed loop system  $F_l(N(s), K(s))$  is then given by

$$F_l(N(s), K(s)) = - \begin{bmatrix} W_{u1}(s)M(s)W_{u2}(s) & W_{u1}(s)M(s)W_{p1}(s) \\ W_{p2}(s)S_o(s)W_{u2}(s) & W_{p2}(s)S_o(s)W_{p1}(s) \end{bmatrix} \quad (2.76)$$

A sufficient conditions for robust performance is thus  $\|F_l(N(s), K(s))\|_\infty < 1$ . Furthermore since

$$\|F_l(N(s), K(s))\|_\infty < 1 \quad (2.77)$$

$$\Leftrightarrow \bar{\sigma} \left( \begin{bmatrix} W_{u1}(j\omega)M(j\omega)W_{u2}(j\omega) & W_{u1}(j\omega)M(j\omega)W_{p1}(j\omega) \\ W_{p2}(j\omega)S_o(j\omega)W_{u2}(j\omega) & W_{p2}(j\omega)S_o(j\omega)W_{p1}(j\omega) \end{bmatrix} \right) < 1 \quad \forall \omega \quad (2.78)$$

$$\Rightarrow \max(\bar{\sigma}(W_{u1}MW_{u2}), \bar{\sigma}(W_{u1}MW_{p1}), \bar{\sigma}(W_{p2}S_oW_{u2}), \bar{\sigma}(W_{p2}S_oW_{p1})) < 1 \quad \forall \omega \quad (2.79)$$

$$\Rightarrow \bar{\sigma}(W_{u1}(j\omega)M(j\omega)W_{u2}(j\omega)) < 1, \quad \bar{\sigma}(W_{p2}(j\omega)S_o(j\omega)W_{p1}(j\omega)) < 1 \quad \forall \omega \quad (2.80)$$

the robust performance condition will imply both robust stability and nominal performance. However, due to the off-diagonal elements in  $F_l(N(s), K(s))$ , the robust performance criterion may be conservative in the general case. If the weighting functions  $W_{p1}(s)$  and  $W_{u2}(s)$  are restricted to scalar transfer functions multiplied with a unity matrix of appropriate dimension, that is if

$$W_{p1}(s) = w_{p1}(s) \cdot I, \quad W_{u2}(s) = w_{u2}(s) \cdot I \quad (2.81)$$

where  $w_{p1}(s)$  and  $w_{u2}(s)$  are scalar systems, it is possible to show that the sufficient robust performance conditions (2.71) is only slightly conservative. Because of (2.81) the uncertainty weights may be gathered in  $W_{u1}(s)$  and the performance weights in  $W_{p2}(s)$ . The robust performance requirement can then be written

$$\bar{\sigma}(F_l(N(j\omega), K(j\omega))) < 1 \quad \forall \omega \quad (2.82)$$

$$\Leftrightarrow \bar{\sigma} \left( \begin{bmatrix} W_{u1}(j\omega)M(j\omega) & W_{u1}(j\omega)M(j\omega) \\ W_{p2}(j\omega)S_o(j\omega) & W_{p2}(j\omega)S_o(j\omega) \end{bmatrix} \right) < 1 \quad \forall \omega \quad (2.83)$$

$$\Leftrightarrow \bar{\sigma} \left( \begin{bmatrix} W_{u1}(j\omega)M(j\omega) \\ W_{p2}(j\omega)S_o(j\omega) \end{bmatrix} \right) < \frac{1}{\sqrt{2}} \quad \forall \omega \quad (2.84)$$

$$\Leftarrow \max\{\bar{\sigma}(W_{u1}(j\omega)M(j\omega)), \bar{\sigma}(W_{p2}(j\omega)S_o(j\omega))\} < \frac{1}{2} \quad \forall \omega \quad (2.85)$$

The inequality (2.84) follows since

$$\bar{\sigma} \left( \begin{bmatrix} W_{u1}(j\omega)M(j\omega) & W_{u1}(j\omega)M(j\omega) \\ W_{p2}(j\omega)S_o(j\omega) & W_{p2}(j\omega)S_o(j\omega) \end{bmatrix} \right) = \sqrt{2}\bar{\sigma} \left( \begin{bmatrix} W_{u1}(j\omega)M(j\omega) \\ W_{p2}(j\omega)S_o(j\omega) \end{bmatrix} \right) \quad (2.86)$$

Thus (2.85) becomes a sufficient condition for robust performance. Consequently if the nominal performance and robust stability criterions are satisfied with some margin – namely a factor 2 – robust performance will be guaranteed. In other words, for an additive uncertainty and nominal performance specification restricted as in (2.81), robust performance can **not** be arbitrarily poor if nominal performance and robust stability is obtained. Fully equivalent results can be found for output multiplicative uncertainty.

**Example 2.3 (Robust Performance Problem II)** Now let us assume a standard performance specification as in Example 2.2 but an input multiplicative robust stability specification on the input complementary sensitivity  $T_i(s)$ , see Table 2.1. We may rewrite this as an additive perturbation simply by multiplying  $W_{u2}(s)$  in Example 2.2 with the plant transfer function  $G(s)$ . The robust performance condition then becomes

$$\bar{\sigma}(F_l(N(j\omega), K(j\omega))) < 1 \quad \forall \omega \quad (2.87)$$

$$\Leftrightarrow \bar{\sigma} \left( \begin{bmatrix} W_{u1}(j\omega)M(j\omega)G(j\omega)W_{u2}(j\omega) & W_{u1}(j\omega)M(j\omega)W_{p1}(j\omega) \\ W_{p2}(j\omega)S_o(j\omega)G(j\omega)W_{u2}(j\omega) & W_{p2}(j\omega)S_o(j\omega)W_{p1}(j\omega) \end{bmatrix} \right) < 1 \quad \forall \omega \quad (2.88)$$

Note that  $M(s)G(s) = T_i(s)$ . Again, due to the off-diagonal elements in  $F_l(N(s), K(s))$ , the condition (2.88) may be conservative. In fact, even if the weightings are restricted as in (2.81) it will be shown that (2.88) may be arbitrarily conservative. With weightings restricted as in (2.81) note that the robust stability criterion becomes

$$\bar{\sigma}(W_{u1}(j\omega)M(j\omega)G(j\omega)) < 1 \quad \forall \omega \quad (2.89)$$

$$\Leftarrow \bar{\sigma}(W_{u1}(j\omega)M(j\omega)\bar{\sigma}(G(j\omega))) < 1 \quad \forall \omega \quad (2.90)$$

$$\Leftrightarrow \bar{\sigma}(\bar{\sigma}(G(j\omega))W_{u1}(j\omega)M(j\omega)) < 1 \quad \forall \omega \quad (2.91)$$

which corresponds to robust stability for an additive perturbation  $\Delta(s)\bar{\sigma}(G(s))W_{u1}(s)$ . Thus if the system is stable for the additive perturbation  $\Delta(s)\bar{\sigma}(G(s))W_{u1}(s)$  it will also be stable for the input multiplicative

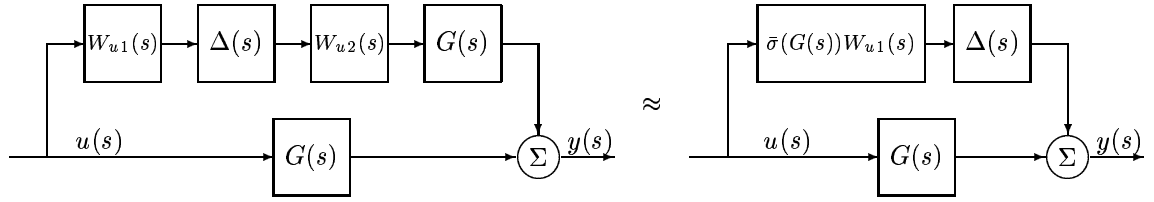


Figure 2.8: Approximating  $G(s)$  with its largest singular value in the uncertainty specification.

perturbation  $\Delta(s)W_{u1}(s)$ . Notice that this corresponds to approximating  $G(s)$  with its largest singular value and moving it to the uncertainty input weight  $W_{u1}(s)$ , see Figure 2.8.

A sufficient condition for robust performance is then

$$\bar{\sigma}(F_l(N(j\omega), K(j\omega))) < 1 \quad \forall \omega \quad (2.92)$$

$$\Leftrightarrow \bar{\sigma} \left( \begin{bmatrix} \bar{\sigma}(G(j\omega))W_{u1}(j\omega)M(j\omega) & \bar{\sigma}(G(j\omega))W_{u1}(j\omega)M(j\omega) \\ W_{p2}(j\omega)S_o(j\omega) & W_{p2}(j\omega)S_o(j\omega) \end{bmatrix} \right) < 1 \quad \forall \omega \quad (2.93)$$

$$\Leftrightarrow \bar{\sigma} \left( \begin{bmatrix} \bar{\sigma}(G(j\omega))W_{u1}(j\omega)M(j\omega) \\ W_{p2}(j\omega)S_o(j\omega) \end{bmatrix} \right) < \frac{1}{\sqrt{2}} \quad \forall \omega \quad (2.94)$$

$$\Leftrightarrow \begin{cases} \bar{\sigma}(G(j\omega))\bar{\sigma}(W_{u1}(j\omega)T_i(j\omega)G^{-1}(j\omega)) < \frac{1}{2} & \forall \omega \\ \bar{\sigma}(W_{p2}(j\omega)S_o(j\omega)) < \frac{1}{2} & \forall \omega \end{cases} \quad (2.95)$$

$$\Leftrightarrow \begin{cases} \frac{\bar{\sigma}(G(j\omega))}{\underline{\sigma}(G(j\omega))}\bar{\sigma}(W_{u1}(j\omega)T_i(j\omega)) < \frac{1}{2} & \forall \omega \\ \bar{\sigma}(W_{p2}(j\omega)S_o(j\omega)) < \frac{1}{2} & \forall \omega \end{cases} \quad (2.96)$$

$$\Leftrightarrow \begin{cases} \bar{\sigma}(W_{u1}(j\omega)T_i(j\omega)) < \frac{1}{2\kappa(G(j\omega))} & \forall \omega \\ \bar{\sigma}(W_{p2}(j\omega)S_o(j\omega)) < \frac{1}{2} & \forall \omega \end{cases} \quad (2.97)$$

Thus (2.97) becomes a sufficient condition for robust performance. Inequality (2.97) shows that even when nominal performance and robust stability are satisfied with reasonable margin, the (sufficient) robust performance criterion can be violated by an arbitrarily large amount if the plant is ill-conditioned. On the other hand, if  $\kappa(G(j\omega)) \approx 1, \forall \omega$ , robust performance can not be arbitrarily poor if nominal performance and robust stability are obtained.

## 2.5 Computing the $\mathcal{H}_\infty$ Optimal Controller

Let us finally briefly present a solution to the  $\mathcal{H}_\infty$  optimal control problem. The problem of solving minimizations of the form

$$K(s) = \inf_{K(s) \in \text{cal}K} \|F_l(N(s), K(s))\|_\infty \quad (2.98)$$

was probably the single most important research area within the automatic control community in the 1980'ies. Probably thousands of papers was published on this particular problem. At first, only algorithms that produced  $\infty$  optimal controllers of very high order were available, see e.g. [13]. For polynomial systems numerical algorithms were available which provided  $\mathcal{H}_\infty$  optimal controllers of the same order as the augmented plant  $N(s)$ . However, the numerics were only efficient for scalar systems. Then in early 1988, Doyle, Glover, Khargonekar and Francis announced an state-space  $\mathcal{H}_\infty$  solution which, like the LQG solution, involved only two Ricatti equations and yielded a controller with the same order as the generalized plant. The results were presented at the 1988 American Control Conference and in the 1989 IEEE paper [14]. This was a major breakthrough for  $\mathcal{H}_\infty$  control theory. The parallels now apparent between  $\mathcal{H}_\infty$  and LQG theory are pervasive. Both controllers have a state estimator-state feedback structure, two Ricatti equations provides the full state feedback matrix  $K_c$  and the output injection matrix  $K_f$  in the estimator, respectively. The paper [14] is now known simply as the DGKF paper.

Given a block  $2 \times 2$  system  $N(s)$  like in Figure 2.3 and a required upper bound  $\gamma$  on the closed loop infinity norm  $\|F_l(N(s), K(s))\|_\infty$  the solution returns a parameterization – which we will denote the DGKF Parameterization –  $K(s) = F_l(J(s), Q(s))$  of all stabilizing controllers such that  $\|F_l(N(s), K(s))\|_\infty < \gamma$ . Any stable transfer function matrix  $Q(s)$  satisfying  $\|Q(s)\|_\infty < \gamma$  will stabilize the closed loop system and cause  $\|F_l(N(s), K(s))\|_\infty < \gamma$ . Any  $Q(s)$  which is unstable or has  $\|Q(s)\|_\infty > \gamma$  will destabilize the closed loop system, or cause  $\|F_l(N(s), K(s))\|_\infty > \gamma$  or both. The solution is provided by the following theorem.

**Theorem 2.6 ( $\mathcal{H}_\infty$ -Suboptimal Control Problem)** *Let  $N(s)$  be given by its state-space matrices  $A$ ,  $B$ ,  $C$  and  $D$  and introduce the notation:*

$$N(s) = \left[ \begin{array}{c|cc} A & B_1 & B_2 \\ \hline C_1 & D_{11} & D_{12} \\ C_2 & D_{21} & D_{22} \end{array} \right] \quad (2.99)$$

Make the following assumptions:

1.  $(A, B_1)$  and  $(A, B_2)$  are stabilizable.
2.  $(C_1, A)$  and  $(C_2, A)$  are detectable.
3.  $D_{12}^T D_{12} = I$  and  $D_{21} D_{21}^T = I$ .
4.  $D_{11} = D_{22} = 0$ .

Solve the two Ricatti equations:

$$X = \text{Ric} \left[ \begin{array}{cc|c} A - B_2 D_{12}^T C_1 & \gamma^{-2} B_1 B_1^T - B_2 B_2^T & \\ \hline -C_1^T (I - D_{12} D_{12}^T)^T (I - D_{12} D_{12}^T) C_1 & & - (A - B_2 D_{12}^T C_1)^T \end{array} \right] \quad (2.100)$$

$$Y = \text{Ric} \left[ \begin{array}{c|cc} (A - B_1 D_{21}^T C_2)^T & \gamma^{-2} C_1^T C_1 - C_2^T C_2 & \\ \hline -B_1 (I - D_{21}^T D_{21}) (I - D_{21}^T D_{21})^T B_1^T & & - (A - B_1 D_{21}^T C_2) \end{array} \right] \quad (2.101)$$

Form the state feedback matrix  $K_c$ , the output injection matrix  $K_f$  and the matrix  $Z$ :

$$K_c = (D_{12}^T C_1 + B_2^T X) \quad (2.102)$$

$$K_f = (B_1 D_{21}^T + Y C_2^T) \quad (2.103)$$

$$Z = (I - \gamma^{-2} Y X)^{-1} \quad (2.104)$$

If  $X \geq 0$  and  $Y \geq 0$  exist and if the spectral radius  $\rho(XY) < \gamma^2$ , then the  $\mathcal{H}_\infty$  DGKF Parameterization is given by:

$$J(s) = \left[ \begin{array}{cc|cc} A - B_2 K_c + \gamma^{-2} B_1 B_1^T X - Z K_f (C_2 + \gamma^{-2} D_{21} B_1^T X) & Z K_f & Z (B_2 + \gamma^{-2} Y C_1^T D_{12}) & \\ \hline -K_c & 0 & I & \\ - (C_2 + \gamma^{-2} D_{21} B_1^T X) & I & 0 & \end{array} \right] \quad (2.105)$$

$$= \left[ \begin{array}{cc} J_{11}(s) & J_{12}(s) \\ J_{21}(s) & J_{22}(s) \end{array} \right] \quad (2.106)$$

Stabilizing controllers  $K(s)$  may now be constructed by connecting  $J(s)$  to any stable transfer function matrix  $Q(s)$  with  $\|Q(s)\|_\infty < \gamma$ :

$$K(s) = F_l(J(s), Q(s)) = J_{11}(s) + J_{12}(s)Q(s) (I - J_{22}(s)Q(s))^{-1} J_{21}(s) \quad (2.107)$$

The  $\infty$ -norm of the closed loop system  $F_l(N(s), F_l(J(s), Q(s)))$  satisfy:

$$\|F_l(N(s), F_l(J(s), Q(s)))\|_\infty < \gamma \quad (2.108)$$

The controller obtained for  $Q(s) = 0$  is known as the central  $\mathcal{H}_\infty$  controller.



Notice that Theorem 2.6 does not provide the optimal  $\mathcal{H}_\infty$  control law. Rather it provides a control law satisfying  $\|F_l(N(s), K(s))\|_\infty < \gamma$  after  $\gamma$  has been specified, provided that a control law exists which can do this. Consequently the designer must iterate on  $\gamma$  to approach the optimal  $\infty$ -norm  $\gamma_0$ . This is different to the LQG-optimal control problem where the optimal solution is found without iteration. The central controller obtained for  $Q(s) = 0$  is not generally the controller achieving the smallest  $\infty$ -norm of the closed loop system. However, since it is a valid controller, given the desired bound  $\gamma$ , it is customary to choose this particular controller for implementation. Specifically, in the commercially available software [15, 2], this is the controller returned by the  $\mathcal{H}_\infty$  control synthesis algorithms.

## 2.6 Conclusions

Let us recapitulate our results so far.

- Robust performance implies both nominal performance and robust stability. Consequently, in general, our design objective should be robust performance.
- Given any of the unstructured complex perturbations introduced in Section 2.3 the closed loop system may be rewritten in  $P\Delta$  form as in Figure 2.4. Then, assuming that every plant in the set described by  $\Delta(s)$  with  $\bar{\sigma}(\Delta) \leq 1$  can occur in practice,  $\|P(s)\|_\infty < 1$  is a non-conservative condition for robust stability.
- The robust performance problem can be assessed by augmenting the robust stability problem with a full complex performance block.
- Assuming a performance specification of the form (2.20) and either an additive or output multiplicative perturbation model, an sufficient  $\mathcal{H}_\infty$  condition for robust performance can be derived which is only slightly conservative provided certain restrictions on the uncertainty and performance weightings are enforced.
- On the other hand, if robustness to input multiplicative uncertainty is required, the  $\mathcal{H}_\infty$  condition for robust performance may be arbitrarily conservative if the plant is ill-conditioned.

Notice that even though the robust stability criterion (2.45) is non-conservative, in formulating the controller synthesis as a  $2 \times 2$  block problem some conservatism will always be introduced when robust performance is considered. For standard additive and output multiplicative uncertainty, the robust performance condition will be reasonably tight, namely up to a factor 2. This applies also for standard input multiplicative uncertainty *provided the plant is well-conditioned*. For ill-conditioned plants, robust performance may be arbitrarily poor even though nominal performance and robust stability are obtained. In other words, for ill-conditioned plants the closed loop properties at the plant input may be very different from those at the plant output. For example, the robustness to output multiplicative uncertainty may be satisfactory even though the robustness to input multiplicative uncertainty is very poor.

Generally it can be concluded, that if an unstructured complex perturbation model is tight, that is if all plants included by the perturbation structure can occur in practice, and if the plant is reasonably well-conditioned, the optimal  $\mathcal{H}_\infty$  controller will not be very conservative in the sense that robust performance will not be arbitrarily poor given nominal performance and robust stability.

On the other hand, if an unstructured complex perturbation model is conservative or if the plant is ill-conditioned, an  $2 \times 2$  block problem  $\mathcal{H}_\infty$  optimal controller may be very conservative. In such cases much is to be gained by a  $\mu$  approach. In the next section robust control design with structured singular values will be considered.

## 3 Robust Control Design using Structured Singular Values

Gathering the analysis tools presented in Section 2, a general framework for robustness analysis of linear systems can be illustrated as in Figure 3.1. Any linear interconnection of control inputs  $u$ , measured outputs  $y$ , disturbances  $d'$ , controlled outputs (error signals)  $e'$ , perturbations  $w$  and a controller  $K$  can be expressed within this framework. In Section 2 we assumed that  $\Delta(s)$  was a full complex block. Now

we will relax this assumption. Here  $\Delta(s)$  is assumed to have a block diagonal structure so as to include a much larger class of uncertainty descriptions, like e.g. parametric uncertainty, see e.g. [3].

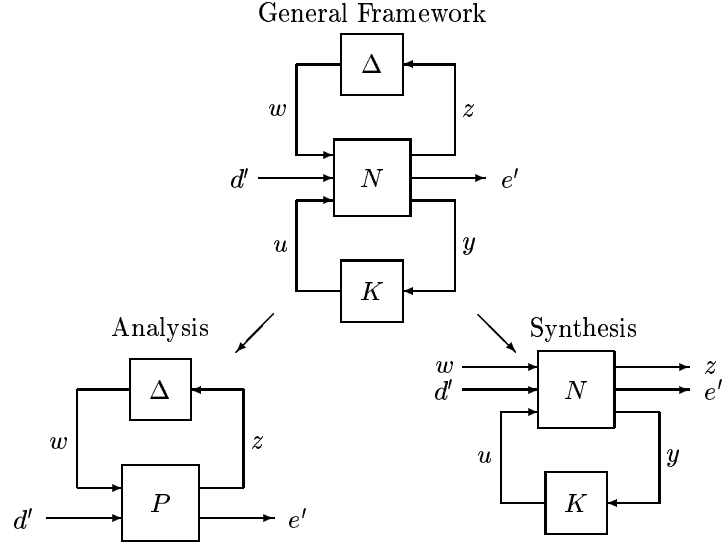


Figure 3.1: A general framework for analysis and synthesis of linear control systems.

Within the general framework analysis and synthesis constitutes two special cases as illustrated in Figure 3.1. Like the  $2 \times 2$  block problem, scalings and weights are conventionally absorbed into the transfer function  $N$  in order to normalize  $d'$ ,  $e'$  and  $\Delta(s)$  to norm 1. Notice that if we partition  $P(s)$  into four blocks consistent with the dimensions of the two input ( $w$ ,  $d'$ ) and two output ( $z$ ,  $e'$ ) vectors we can identify  $P_{11}(s)$  as the transfer matrix  $P(s)$  in Figure 2.4.

### 3.1 $\mu$ Analysis

Assume that  $\Delta(s)$  is a member of the bounded subset:

$$\mathbf{B}\Delta = \{\Delta(s) \in \Delta \mid \bar{\sigma}(\Delta(j\omega)) < 1\} \quad (3.1)$$

where  $\Delta$  is defined by:

$$\Delta = \left\{ \text{diag} \left( \delta_1^r I_{r_1}, \dots, \delta_{m_r}^r I_{r_{m_r}}, \delta_1^c I_{r_{m_r+1}}, \dots, \delta_{m_c}^c I_{r_{m_r+m_c}}, \Delta_1, \dots, \Delta_n \right) \mid \delta_i^r \in \mathbf{R}, \right. \\ \left. \delta_i^c \in \mathbf{C}, \Delta_j \in \mathbf{C}^{r_{m_r+m_c+j} \times r_{m_r+m_c+j}} \right\} \quad (3.2)$$

Clearly, the block diagonal structure on  $\Delta$  allows much more detailed uncertainty models compared with the  $\mathcal{H}_\infty$  approach where  $\Delta(s)$  is simply a full complex block. Notice that this is of course just a special element of the above set  $\Delta$ . Define also the *corresponding complex perturbation set*  $\Delta_c$ :

$$\Delta_c = \left\{ \text{diag} \left( \delta_1^c I_{r_1}, \dots, \delta_{m_r+m_c}^c I_{r_{m_r+m_c}}, \Delta_1, \dots, \Delta_n \right) \mid \delta_i^c \in \mathbf{C}, \Delta_j \in \mathbf{C}^{r_{m_r+m_c+j} \times r_{m_r+m_c+j}} \right\} \quad (3.3)$$

which we will use in connection with mixed  $\mu$  synthesis. Robust stability under structured perturbations  $\Delta(s) \in \mathbf{B}\Delta$  is determined by the following theorem which is an extension of Theorem 2.4.

**Theorem 3.1** *Assume that the interconnection  $P_{11}(s)$  is stable and that the perturbation  $\Delta(s)$  is of such a form that the perturbed closed loop system is stable if and only if the map of  $\det(I - P_{11}(s)\Delta(s))$  as  $s$  traverses the Nyquist  $\mathcal{D}$  contour does not encircle the origin. Then the closed loop system in Figure 3.1 is stable for all perturbations  $\Delta(s) \in \mathbf{B}\Delta$  if and only if*

$$\det(I - P_{11}(j\omega)\Delta(j\omega)) \neq 0 \quad \forall \omega, \forall \Delta(j\omega) \in \mathbf{B}\Delta \quad (3.4)$$

$$\Leftrightarrow \rho(P_{11}(j\omega)\Delta(j\omega)) < 1 \quad \forall \omega, \forall \Delta(j\omega) \in \mathbf{B}\Delta \quad (3.5)$$

$$\Leftrightarrow \bar{\sigma}(P_{11}(j\omega)) < 1 \quad \forall \omega \quad (3.6)$$

**Proof of Theorem 3.1** The proof follows easily from Theorem 2.4 with  $\Delta(s) \in \mathbf{B}\Delta$ .  $\square$

Note that (3.6) is only a sufficient condition for robust stability. The necessity of the similar condition (2.44) for unstructured perturbations follows from the fact that the unstructured perturbation set include *all*  $\Delta(s)$  with  $\bar{\sigma}(\Delta(j\omega)) \leq 1$ . Here, however, we restrict the set of perturbations to  $\Delta(s) \in \mathbf{B}\Delta$  and therefore, in general, condition (3.6) can be arbitrarily conservative. Rather than a singular value constraint we need some measure which takes into account the structure of the perturbations  $\Delta(s)$ . This is precisely the structured singular value  $\mu$ .

Given a matrix  $P \in \mathbf{C}^{n \times m}$ , the positive real-valued function  $\mu$  is then defined by:

$$\mu_{\Delta}(P) \triangleq \frac{1}{\min \{ \bar{\sigma}(\Delta) : \Delta \in \Delta, \det(I - P\Delta) = 0 \}} \quad (3.7)$$

unless no  $\Delta \in \Delta$  makes  $I - P\Delta$  singular, in which case  $\mu_{\Delta}(P) = 0$ . Thus  $1/\mu_{\Delta}(P)$  is the ‘‘size’’ of the smallest perturbation  $\Delta$ , measured by its maximum singular value, which makes  $\det(I - P\Delta) = 0$ . Equivalently,  $1/\mu_{\Delta}(P(j\omega))$  is the size of the smallest perturbation  $\Delta(j\omega)$  which shifts the characteristic loci of the transfer matrix  $P(s)$  to the Nyquist point  $-1$  at the frequency  $\omega$ .

From the definition of  $\mu$  and Theorem 3.1 we now have the following theorem for assessing robust stability, see also [16, 17]:

**Theorem 3.2 (Robust Stability with  $\mu$ )** *Assume that the interconnection  $P_{11}(s)$  is stable and that the perturbation  $\Delta(s)$  is of such a form that the perturbed closed loop system is stable if and only if the map of  $\det(I - P_{11}(s)\Delta(s))$  as  $s$  traverses the Nyquist  $\mathcal{D}$  contour does not encircle the origin. Then the closed loop system in Figure 3.1 is stable for all perturbations  $\Delta(s) \in \mathbf{B}\Delta$  if and only if :*

$$\|\mu_{\Delta}(P_{11}(s))\|_{\infty} \leq 1 \quad (3.8)$$

where:

$$\|\mu_{\Delta}(P_{11}(s))\|_{\infty} \triangleq \sup_{\omega} \mu_{\Delta}(P_{11}(j\omega)) \quad (3.9)$$

For robust performance the transfer function  $F_u$  from  $d'$  to  $e'$  may be partitioned as a linear fractional transformation:

$$e'(s) = F_u(P(s), \Delta(s))d'(s) = \left[ P_{22}(s) + P_{21}(s)\Delta(s)(I - P_{11}(s)\Delta(s))^{-1}P_{12}(s) \right] d'(s) \quad (3.10)$$

Here  $P_{22}(s)$  is the weighted nominal performance function and  $F_u(P(s), \Delta(s))$  is thus the weighted perturbed performance function. Now from (3.10) the robust performance objective becomes

$$\|F_u(P(s), \Delta(s))\|_{\infty} = \sup_{\omega} \bar{\sigma}(F_u(P(j\omega), \Delta)) < 1 \quad (3.11)$$

As in Section 2.4 we notice that the condition for robust performance is a singular value constraint similar to the robust stability condition (2.44) and conclude: *the robust performance objective (3.11) is satisfied if and only if the interconnection  $F_u(P(s), \Delta(s))$  is robustly stable for a norm bounded matrix perturbation  $\Delta_p(s)$  with  $\bar{\sigma}(\Delta_p(j\omega)) \leq 1$* . Hence by augmenting the perturbation structure with a full complex performance block  $\Delta_p(s)$  the robust performance condition can be equivalenced with a robust stability condition, see Figure 2.7.

We thus have the following theorem for assessing robust performance, see [16, 17]:

**Theorem 3.3 (Robust Performance with  $\mu$ )** *Let an  $\mathcal{H}_{\infty}$  performance specification be given on the transfer function from  $d'$  to  $e'$  – typically a weighted sensitivity specification – of the form:*

$$\|F_u(P(s), \Delta(s))\|_{\infty} = \sup_{\omega} \bar{\sigma}(F_u(P(j\omega), \Delta(j\omega))) < 1 \quad (3.12)$$

*Then  $F_u(P(s), \Delta(s))$  is stable and  $\|F_u(P(s), \Delta(s))\|_{\infty} < 1, \forall \Delta(s) \in \mathbf{B}\Delta$  if and only if*

$$\|\mu_{\tilde{\Delta}}(P(s))\|_{\infty} \leq 1 \quad (3.13)$$

*where the perturbation set is augmented with a full complex performance block:*

$$\tilde{\Delta} = \{ \text{diag}(\Delta, \Delta_p) \mid \Delta \in \Delta, \Delta_p \in \mathbf{C}^{k \times k} \} \quad (3.14)$$

Theorem 3.3 is the real payoff for measuring performance in terms of the  $\infty$ -norm and bounding model uncertainty in the same manner. Using  $\mu$  it is then possible to test for both robust stability and robust performance in a non-conservative manner. Indeed, if the uncertainty is modeled exactly by  $\Delta(s)$  – i.e., if all plants in the norm-bounded set can really occur in practice, then the  $\mu$  condition for robust performance is necessary and sufficient. Notice how the  $\mu$  theorems provides much tighter conditions for robust performance compared with the  $\mathcal{H}_\infty$  results in Section 2.4. Performance and stability conditions are now separated, much tighter uncertainty descriptions may be given due to the diagonal structure on  $\Delta$  and non-conservative results are provided for all perturbation models and even for ill-conditioned systems.

Since  $\Delta_1 = \text{diag}\{\Delta, 0\}$  and  $\Delta_p = \text{diag}\{0, \Delta_p\}$  are special cases of  $\Delta \in \tilde{\Delta}$  it is clear that

$$\mu_{\tilde{\Delta}}(P(j\omega)) \geq \max\{\mu_{\Delta}(P_{11}(j\omega)), \mu_{\Delta_p}(P_{22}(j\omega)) = \bar{\sigma}(P_{22}(j\omega))\} \quad (3.15)$$

which implies that for robust performance it is necessary that the closed loop system is robustly stable and satisfies the nominal performance objective.

### 3.2 Computation of $\mu$

Unfortunately Equation (3.7) is not suitable for computing  $\mu$  since the implied optimization problem may have multiple local maxima [16, 18]. However tight upper and lower bounds for  $\mu$  may be effectively computed for both complex and mixed perturbations sets. Algorithms for computing these bounds have been documented in several papers, see e.g. [16, 19]. For simplicity assume that  $P \in \mathbf{C}^{n \times n}$  is square. Define  $\beta_{min}$  as:

$$\beta_{min} = \inf_{\beta \in \mathbf{R}_+, G \in \mathbf{G}, D \in \mathbf{D}} \left\{ \beta \left| \bar{\sigma} \left[ \left( \frac{DPD^{-1}}{\beta} - jG \right) (I + G^2)^{-\frac{1}{2}} \right] \leq 1 \right. \right\} \quad (3.16)$$

then

$$\max_{Q \in \mathbf{Q}} \rho(QP) \leq \mu_{\Delta}(P) \leq \beta_{min} \quad (3.17)$$

Here  $\mathbf{Q}$  is the set:

$$\mathbf{Q} = \left\{ Q \in \Delta \mid \delta_i^r \in [-1; 1], \delta_i^c \delta_i^c = 1, \Delta_j^H \Delta_j = I_{r_{m_r+m_c+j}} \right\} \quad (3.18)$$

where  $(\cdot)^H$  denotes complex conjugate transpose.  $\mathbf{D}$  is the set of hermitian positive definite matrices:

$$\mathbf{D} = \left\{ \text{diag} (D_1, \dots, D_{m_r+m_c}, d_1 I_{r_{m_r+m_c+1}}, \dots, d_n I_{r_m}) \mid D_i \in \mathbf{C}^{r_i \times r_i}, D_i^H = D_i > 0, d_j \in \mathbf{R}, d_j > 0 \right\} \quad (3.19)$$

where  $r_m = r_{m_r+m_c+n}$ . Finally,  $\mathbf{G}$  is the set:

$$\mathbf{G} = \left\{ \text{diag} (G_1, \dots, G_{m_r}, O_{r_{m_r+1}}, \dots, O_{r_m}) \mid G_i \in \mathbf{C}^{r_i \times r_i}, G_i = G_i^H \right\} \quad (3.20)$$

For purely complex perturbation sets ( $G = 0$ ) the above bounds reduce to:

$$\max_{Q \in \mathbf{Q}} \rho(QP) \leq \mu_{\Delta}(P) \leq \inf_{D \in \mathbf{D}} \bar{\sigma} (DPD^{-1}) \quad (3.21)$$

In Equation (3.17) and (3.21) the lower bound is actually an equality [19] but unfortunately the function  $\rho(QM)$  is non-convex so we cannot guarantee to find the global maximum and hence we only obtain a lower bound for  $\mu$ . In this paper the algorithms provided in the MATLAB  *$\mu$ -Analysis and Synthesis Toolbox* were used for computing  $\mu$ -bounds.

### 3.3 $\mu$ Synthesis

For robust synthesis the transfer function  $F_l$  from  $[w \ d']^T$  to  $[z \ e']^T$  may be partitioned as the linear fractional transformation:

$$\begin{bmatrix} z(s) \\ e'(s) \end{bmatrix} = F_l(N(s), K(s)) \begin{bmatrix} w(s) \\ d'(s) \end{bmatrix} = \begin{bmatrix} N_{11}(s) + N_{12}(s)K(s) (I - N_{22}(s)K(s))^{-1} N_{21}(s) \\ N_{21}(s) \end{bmatrix} \begin{bmatrix} w(s) \\ d'(s) \end{bmatrix} \quad (3.22)$$

Noticing that  $F_l(N(s), K(s)) = P(s)$  and using Theorem 3.3 a stabilizing controller  $K(s)$  achieves robust performance if and only if for each frequency  $\omega \in [0, \infty]$ , the structured singular value satisfies:

$$\mu_{\Delta} (F_l(N(j\omega), K(j\omega))) < 1 \quad (3.23)$$

Consequently the robust performance problem becomes one of synthesizing a nominally stabilizing controller  $K(s)$  that minimizes  $\mu_{\Delta} (F_l(N, K))$  across frequency:

$$K(s) = \inf_{K(j\omega) \in \mathcal{K}} \left\| \mu_{\Delta} (F_l(N(s), K(s))) \right\|_{\infty} \quad (3.24)$$

where  $\mathcal{K}$  denotes the set of all nominally stabilizing controllers.

### 3.3.1 Complex $\mu$ Synthesis – D-K Iteration

Unfortunately (3.24) is not tractable since  $\mu$  cannot be directly computed. Rather the upper bound on  $\mu$  is used to formulate the control problem. For purely complex perturbations,  $m_r = 0$  in (3.2), the upper bound problem becomes

$$K(s) = \inf_{K(j\omega) \in \mathcal{K}} \sup_{\omega} \inf_{D(\omega) \in \mathbf{D}} \left\{ \bar{\sigma} (D(\omega) F_l(N(j\omega), K(j\omega)) D^{-1}(\omega)) \right\} \quad (3.25)$$

Unfortunately, it is also not known how to solve (3.25). However an approximation to complex  $\mu$  synthesis can be made by the following iterative scheme. For a fixed controller  $K(s)$ , the problem of finding  $D(\omega)$  is just the complex  $\mu$  upper bound problem which is a convex problem with known solution. Having found these scalings we may fit stable minimum phase transfer function matrices  $D(j\omega)$  to  $D(\omega)$  such that the interconnection  $D(s)N(s)D^{-1}(s)$  is stable. We may impose the extra constraint that the approximations  $D(s)$  should be minimum phase (so that  $D^{-1}(s)$  is stable too) since any phase in  $D(j\omega)$  is absorbed into the complex perturbations. For a given magnitude of  $D(\omega)$ , the phase corresponding to a minimum phase transfer function system may be computed using complex cepstrum techniques. Accurate transfer function estimates may then be generated using standard frequency domain least squares techniques. For given scalings  $D(s)$  the problem of finding a controller  $K(s)$  which minimizes the norm  $\|F_l(D(s)N(s)D^{-1}(s), K(s))\|_{\infty}$  will be reduced to a standard  $\mathcal{H}_{\infty}$  problem. Repeating this procedure, denoted  $D$ - $K$  iteration, several times will yield the complex  $\mu$  optimal controller provided the algorithm converges. Even though the computation of the  $D$  scalings and the optimal  $\mathcal{H}_{\infty}$  controller are both convex problems, the  $D$ - $K$  iteration procedure is *not* jointly convex in  $D(s)$  and  $K(s)$  and counter examples has been given [20]. However,  $D$ - $K$  iteration has been successfully applied to a large number of applications. The  $D$ - $K$  iteration procedure may be outlined as below.

#### Procedure 3.1 (D-K Iteration)

1. Given an augmented system  $N(s)$ , let  $i = 1$  and  $P_i(s) = N(s)$ .
2. Find the  $\mathcal{H}_{\infty}$  optimal controller  $K_i(s)$ :

$$K_i(s) = \inf_{K(s) \in \mathcal{K}} \|F_l(P_i(s), K(s))\|_{\infty} \quad (3.26)$$

3. Find the scalings  $D_{i+1}^*(\omega)$  solving the complex  $\mu$  upper bound problem

$$D_{i+1}^*(\omega) = \inf_{D(\omega) \in \mathbf{D}} \left\{ \bar{\sigma} (D(\omega) F_l(N(s), K_i(s)) D^{-1}(\omega)) \right\} \quad (3.27)$$

*pointwise across frequency  $\omega$ .*

4. Fit a stable minimum phase transfer function matrix  $D_{i+1}(s)$  to the pointwise scalings  $D_{i+1}^*(\omega)$ . Augment  $D_{i+1}(s)$  with a unity matrix of appropriate size such that  $D_{i+1}(s)$  is compatible with  $N(s)$ . Construct the (stable) interconnection  $P_{i+1}(s) = D_{i+1}(s)N(s)D_{i+1}^{-1}(s)$ .
5. Let  $i = i + 1$  and repeat from 2 until no further improvement in  $\mu_{\Delta} (F_l(N(s), K_i))$  can be achieved.

With the release of the MATLAB  $\mu$ -Analysis and Synthesis Toolbox commercially available software now exists to support complex  $\mu$  synthesis using  $D$ - $K$  iteration. The procedure 3.1 may be implemented quite easily with the aid of the toolbox. Notice that an approximation to mixed real and complex  $\mu$  synthesis can be achieved by approximating the mixed perturbation set  $\Delta$  with corresponding complex set  $\Delta_{\mathbf{c}}$ , that is to approximate all real perturbations with complex perturbations.

### 3.3.2 Mixed $\mu$ Synthesis – G,D-K Iteration

The general mixed real and complex  $\mu$  problem is unfortunately much more difficult than the purely complex  $\mu$  problem. For the mixed problem the upper bound problem becomes

$$K(s) = \inf_{K(j\omega) \in \mathcal{K}} \sup_{\omega} \inf_{D(\omega) \in \mathbf{D}, G(\omega) \in \mathbf{G}} \inf_{\beta(\omega) \in \mathbf{R}_+} \{ \beta(\omega) \mid \bar{\sigma}(\Gamma(\omega)) \leq 1 \} \quad (3.28)$$

where

$$\Gamma(\omega) = \left( \frac{D(\omega)F_l(N(j\omega), K(j\omega))D^{-1}(\omega)}{\beta(\omega)} - jG(\omega) \right) (I + G^2(\omega))^{-\frac{1}{2}} \quad (3.29)$$

We will denote this a *direct* upper bound problem emphasizing that the problem is posed directly in line with the way the upper bound is computed. Again no known solution to (3.29) exists. Rather it must be solved iteratively similarly to  $D$ - $K$  iteration. For fixed  $K(s)$  the problem of finding  $D(\omega)$ ,  $G(\omega)$  and  $\beta(\omega)$  is just the mixed  $\mu$  upper bound problem. Having found these scalings we may fix  $\beta^* = \max_{\omega} \beta(\omega)$  and fit transfer function matrices  $D(s)$  and  $G(s)$  to  $D(\omega)$  and  $jG(\omega)$ . It can then be shown, see [5], that, using spectral factorizations, we may form a stable interconnection  $P_{DG}(s)$  which approximates  $\Gamma(\omega)$  across frequency  $\omega$ . For given  $\beta^*$ ,  $D(s)$  and  $G(s)$  the problem of finding the controller  $K(s)$  will be reduced to a standard  $\mathcal{H}_{\infty}$  problem. Unfortunately, for the general upper bound problem the scalings cannot be restricted to be minimum phase since the phase is not absorbed into the (real) perturbations. Thus the scalings must be fitted both in magnitude and phase. For example, we must require that the phase of the diagonal elements of  $G(j\omega)$  is  $90^\circ$  for all frequencies  $\omega$ . The fitting of these purely imaginary diagonal elements can only be obtained using high order all pass structures causing the controller order to explode.

This procedure of iteratively solving Equation (3.29) is usually referred to as  $D, G$ - $K$  iteration. The fact that (3.28) is not a singular value minimization, but rather a minimization subject to a singular value constraint and the fact that the formed augmented system must be stable enforces some minor modifications to the general  $D, G$ - $K$  algorithm. However it will be beyond the scope of this paper to explain these changes in detail. The reader may consult [5]. It can be shown that the resulting  $D, G$ - $K$  iteration is monotonically non-increasing for perfect realizations of the scaling matrices transfer function estimates and thus converges to a local minimum for the mixed  $\mu$  upper bound. Since the minimization is not *jointly* convex in the scaling matrices and  $K$  we cannot guaranty convergence to the global minimum.

Successful results on  $G, D$ - $K$  iteration has been reported for simple mixed  $\mu$  problems, see e.g. [6]. However, the need for fitting purely complex scalings with high order all-pass transfer functions as well as the general need for fitting both in phase and magnitude severely hampers the practical use of  $G, D$ - $K$  iteration for mixed  $\mu$  synthesis.

### 3.3.3 Mixed $\mu$ Synthesis – $\mu$ -K Iteration

As discussed above the general  $D, G$ - $K$  approach for controller synthesis with mixed perturbation sets  $\Delta$  is much more complicated than  $D$ - $K$  iteration for purely complex perturbations. Recently, however, a different approach for mixed  $\mu$  synthesis, denoted  $\mu$ - $K$  iteration, has been proposed which only require the scalings to be fitted in magnitude [7]. This new approach is the subject of this section.

Whereas the  $D, G$ - $K$  approach is a *direct* upper bound minimization,  $\mu$ - $K$  iteration is an *indirect* upper bound minimization in the sense that the augmented system matrix corresponding to  $P_{DG}(s)$  above does not directly reflect the structure of the  $\mu$  upper bound as in (3.29).

The main idea of the proposed  $\mu$ - $K$  iteration scheme is to perform a scaled D-K iteration where the difference between mixed and complex  $\mu$  is taken into account through an additional scaling matrix  $\Gamma(s)$ . The iteration is performed as follows:

#### Procedure 3.2 ( $\mu$ -K Iteration)

1. Given the augmented system  $N(s)$ , let  $\gamma_0(s) = 1$ ,  $D_0(s) = I$  and  $P_0(s)$  be given by

$$P_0(s) = \begin{bmatrix} \gamma_0(s)I_{n_{wd}} & 0 \\ 0 & I_{n_u} \end{bmatrix} D_0(s)N(s)D_0^{-1}(s) = \Gamma_0(s)D_0(s)N(s)D_0^{-1}(s) = N(s). \quad (3.30)$$

$n_{wd} = \dim \{[w; d']\}$  denotes the number of external inputs and  $n_u = \dim \{u\}$  denotes the number of controlled inputs. Let  $K_0(s) = K_1(s)$  be a stabilizing controller, compute the  $\infty$ -norm  $\|F_l(P_0(s), K_0(s))\|_\infty$  and let  $i = 1$ .

2. Compute the mixed and corresponding complex  $\mu$  upper bounds  $\bar{\mu}_{\tilde{\Delta}}(F_l(N(j\omega), K_i(j\omega)))$  and  $\bar{\mu}_{\tilde{\Delta}_c}(F_l(N(j\omega), K_i(j\omega)))$  at each frequency  $\omega$ . Note that the complex  $\mu$  upper bound equals  $\bar{\sigma}(D_i^*(\omega)F_l(N(j\omega), K_i(j\omega))D_i^{*-1}(\omega))$  where the scalings  $D_i^*(\omega)$  are found solving the minimization

$$D_i^*(\omega) = \inf_{D \in \mathbf{D}} \bar{\sigma}(DF_l(N(j\omega), K_i(j\omega))D^{-1}) \quad \forall \omega \geq 0. \quad (3.31)$$

3. Compute  $\beta_i(\omega)$  given by:

$$\beta_i(\omega) = \frac{\bar{\mu}_{\tilde{\Delta}}(F_l(N(j\omega), K_i(j\omega)))}{\bar{\mu}_{\tilde{\Delta}_c}(F_l(N(j\omega), K_i(j\omega)))} \frac{1}{|\gamma_{i-1}(j\omega)|} - 1 \quad (3.32)$$

4. Fit, in magnitude, a stable minimum phase transfer function matrix  $D_i(j\omega)$  to  $D_i^*(\omega)$  across frequency  $\omega$  and augment  $D_i(s)$  with a unity matrix of appropriate size such that  $D_i(s)$  is compatible with  $N(s)$

5. Determine an upper bound for the constant  $\alpha \in [0; 1]$  according to

$$\bar{\alpha}_i(\omega) = \begin{cases} \left( \frac{\|F_l(P_{i-1}(s), K_{i-1}(s))\|_\infty}{\bar{\sigma}(F_l(D_i(j\omega)N(j\omega)D_i^{-1}(j\omega), K_i(j\omega)))} |\gamma_{i-1}(j\omega)|} - 1 \right) \frac{1}{\beta_i(\omega)} & \text{if } \beta_i(\omega) > 0 \\ 1 & \text{if } \beta_i(\omega) \leq 0 \end{cases} \quad (3.33)$$

6. If  $\inf_\omega \bar{\alpha}_i(\omega) > 1$ , let  $\inf_\omega \bar{\alpha}_i(\omega) = 1$ . Choose a constant  $\alpha_i = \kappa \inf_\omega \bar{\alpha}_i(\omega)$  where  $\kappa \in [0; 1]$  and compute

$$\gamma_i^*(\omega) = (1 - \alpha_i)|\gamma_{i-1}(j\omega)| + \alpha_i \frac{\bar{\mu}_{\tilde{\Delta}}(F_l(N(j\omega), K_i(j\omega)))}{\bar{\mu}_{\tilde{\Delta}_c}(F_l(N(j\omega), K_i(j\omega)))}, \quad \forall \omega \geq 0. \quad (3.34)$$

Fit, in magnitude, a stable minimum phase transfer function  $\gamma_i(j\omega)$  to  $\gamma_i^*(\omega)$  across frequency  $\omega$ .

7. Construct

$$P_i(s) = \Gamma_i(s)D_i(s)N(s)D_i^{-1}(s) \quad (3.35)$$

and compute the optimal  $\mathcal{H}_\infty$  controller:

$$K_{i+1}(s) = \inf_{K(s) \in \mathcal{K}} \|F_l(P_i(s), K(s))\|_\infty. \quad (3.36)$$

8. Compute the mixed and corresponding complex  $\mu$  upper bounds  $\bar{\mu}_{\tilde{\Delta}}(F_l(N(j\omega), K_{i+1}(j\omega)))$  and  $\bar{\mu}_{\tilde{\Delta}_c}(F_l(N(j\omega), K_{i+1}(j\omega)))$  at each frequency  $\omega$ .

9. Compute  $\beta_{i+1}(\omega)$  given by:

$$\beta_{i+1}(\omega) = \frac{\bar{\mu}_{\tilde{\Delta}}(F_l(N(j\omega), K_{i+1}(j\omega)))}{\bar{\mu}_{\tilde{\Delta}_c}(F_l(N(j\omega), K_{i+1}(j\omega)))} \frac{1}{|\gamma_i(j\omega)|} - 1 \quad (3.37)$$

10. If  $\sup_\omega |\beta_{i+1}(\omega)| > \sup_\omega |\beta_i(\omega)|$  return to 6 and reduce  $\kappa$ . Otherwise compute  $\|F_l(P_i(s), K_i(s))\|_\infty$  and let  $i = i + 1$ .

11. Repeat from 4 until no further reduction in  $\|\bar{\mu}_{\tilde{\Delta}}(F_l(N(j\omega), K_i(j\omega)))\|_\infty$  can be achieved.

The full  $\mu$ - $K$  iteration procedure may seem somewhat involved. However, the main idea is simple. Given the augmented system  $N(s)$ , the controller found in Step 2 for  $i = 1$  is simply the optimal  $\mathcal{H}_\infty$  controller for  $N(s)$ . We may then compute upper bounds for  $\mu$  across frequency given both the “true” mixed perturbation set  $\tilde{\Delta}$  and the fully complex approximation  $\tilde{\Delta}_c$ . In order to “trick” the  $\mathcal{H}_\infty$  in the next iteration to concentrate more on mixed  $\mu$ , we will construct a system  $P_1(s)$  with frequency response equal to the mixed  $\mu$  upper bound just computed. This is fully equivalent to  $D, G$ - $K$  iteration. In  $\mu$ - $K$  iteration,

however, the structure of the approximation is different.  $P_1(s)$  is constructed by applying two scalings to the original system  $N(s)$ . A  $D$  scaling such that  $\bar{\sigma}(P_1(j\omega))$  approximates the complex  $\mu$  upper bound and a  $\Gamma$  scaling to shift from complex to mixed  $\mu$ . Assume perfect realizations of the  $D$  and  $\Gamma$  scalings and that we may choose  $\alpha_1 = 1$ . Then

$$\bar{\sigma}(F_l(P_1(j\omega), K_1(j\omega))) = F_l(\Gamma_1(j\omega)D_1(j\omega)N(j\omega)D_1^{-1}(j\omega), K_1(j\omega)) \quad (3.38)$$

$$= |\gamma_1(j\omega)|\bar{\sigma}(F_l(D_1(j\omega)N(j\omega)D_1^{-1}(j\omega), K_1(j\omega))) \quad (3.39)$$

$$= |\gamma_1(j\omega)|\bar{\mu}_{\bar{\Delta}_c}(F_l(N(j\omega), K_1(j\omega))) \quad (3.40)$$

$$= \bar{\mu}_{\bar{\Delta}}(F_l(N(j\omega), K_1(j\omega))) \quad \text{for } \alpha_1 = 1 \quad (3.41)$$

and the controller  $K_2(s)$  will minimize the  $\infty$ -norm of an augmented system which closed with the previous controller  $K_1(s)$  had maximum singular value approximating mixed  $\mu$ . New mixed and complex  $\mu$  bounds may then be computed and the procedure may be repeated. Unfortunately it is not possible to choose  $\alpha_i = 1$  in general since we may then suffer from ‘‘pop-up’’ type phenomena, where for some frequencies a small increase in the maximum singular value of  $P_i(s)$  creates a very large increase in  $\mu$ . This type of behavior is unfortunately possible with mixed  $\mu$  problems. However by reducing  $\alpha$ , that is by filtering  $\gamma$  through a stable first order filter, the ‘‘pop-up’’ type phenomena may be avoided with proper choice of  $\alpha$ . In  $D, G$ - $K$  iteration the absence of ‘‘pop-up’’ type phenomena are ensured by the choice  $\beta^* = \max_{\omega} \beta(\omega)$ , see [5].

We then have the following lemma:

**Lemma 3.1** *The  $\mu$ - $K$  iteration procedure described above is monotonically non-increasing in  $\|F_l(P_i(s), K_i(s))\|_{\infty}$  given perfect realizations of the  $D(s)$  and  $\gamma(s)$  scalings. Provided  $\|\beta(\omega)\|_{\infty}$  converges to zero the procedure will converge to a local minimum for  $\|\bar{\mu}_{\bar{\Delta}}(F_l(N(j\omega), K_i(j\omega)))\|$ .*

**Proof of Lemma 3.1** As noticed above, the  $\bar{\sigma}(F_l(P_i(s), K_i(s)))$  equals the upper bound  $\bar{\mu}_{\bar{\Delta}}(F_l(N(s), K_i(s)))$  for perfect realizations of the scalings  $\gamma_i(s)$  and  $D_i(s)$  and for  $\alpha_i = 1$ . For  $\alpha_i \neq 1$  this is not true. However if

$$|\gamma_{i-1}(j\omega)| \rightarrow \frac{\bar{\mu}_{\bar{\Delta}}(F_l(N(j\omega), K_i(j\omega)))}{\bar{\mu}_{\bar{\Delta}_c}(F_l(N(j\omega), K_i(j\omega)))} \quad (3.42)$$

then from (3.34) and perfect realization of  $\gamma_i(j\omega)$ :

$$|\gamma_{i-1}(j\omega)| \rightarrow |\gamma_i(j\omega)| \quad (3.43)$$

and it is clear that

$$\bar{\sigma}(F_l(\Gamma_i(j\omega)D_i(j\omega)N(j\omega)D_i^{-1}(j\omega), K_i(j\omega))) \rightarrow \bar{\mu}_{\bar{\Delta}}(F_l(N(j\omega), K_i(j\omega))). \quad (3.44)$$

Notice that Equation (3.42) implies that  $\beta_i(\omega) \rightarrow 0$ . Thus in order to reach a local minimum for  $\|\bar{\mu}_{\bar{\Delta}}(F_l(N(s), K(s)))\|_{\infty}$  we must fulfill the following two criteria

1. The iteration must be monotonically non-increasing in  $\|F_l(P_i(s), K_i(s))\|_{\infty}$ , that is

$$\|F_l(P_i(s), K_i(s))\|_{\infty} \leq \|F_l(P_{i-1}(s), K_{i-1}(s))\|_{\infty} \quad \forall i. \quad (3.45)$$

2. Furthermore the iteration must be monotonically non-increasing in  $\|\beta_i(\omega)\|_{\infty}$ , that is

$$\|\beta_i(\omega)\|_{\infty} \leq \|\beta_{i-1}(\omega)\|_{\infty} \quad \forall i. \quad (3.46)$$

In Appendix A it is shown that the criteria (3.45) can be met by choosing  $\bar{\alpha}_i(\omega)$  as in (3.33). If  $\kappa$  then can be chosen to fulfill the criteria (3.46) the iteration will converge to a local minimum for  $\|\bar{\mu}_{\bar{\Delta}}(F_l(N(s), K(s)))\|_{\infty}$ .  $\square$

Numerical evidence suggests that  $\kappa$  can indeed be chosen to fulfill (3.46). However, it is likely that examples may be constructed where no  $\kappa$  fulfilling (3.46) can be found. Notice that for  $\alpha = 0$ ,  $\forall i$ ,  $\mu$ - $K$  iteration will reduce to standard  $D$ - $K$  iteration and only the criteria (3.45) will be considered in the iteration. If  $\beta_i(\omega) > 0$ , for some  $\omega$ , then for  $\kappa = 1$  it can be shown, see Appendix A, that

$$\|F_l(P_i(s), K_i(s))\|_{\infty} = \|P_{i-1}(s), K_{i-1}(s)\|_{\infty}. \quad (3.47)$$

Thus in this situation, only the criteria (3.46) will be considered in the  $i$ 'th step of the iteration. By choosing  $\alpha$  (or  $\kappa$ ) in between these two extremes, we may attempt to fulfill both criteria (3.45) and (3.46).



## 4 Examples

Now two design studies will be presented illustrating the  $\mu$  techniques given in the previous section. One example considers control of an idealized C.D. player servo and is taken from [21]. The other example deals with the control of a multivariable ( $2 \times 2$ ) water tank system, where the control problem can be formulated as to maintain a specified level and temperature in the tank for a range of operating points and effluent mass flows.

### 4.1 C.D. Player Servo

The servo arm for a computer disc drive or a compact disc player is essentially a small flexible structure, whose dynamics will depend on various physical quantities. Provided the product is to be mass produced, the control design for the servo should work for any product from the assembly line and thus the design should be insensitive to variations in the parameters of the servo model.

Here a very simple idealized model of the servo is considered. The control problem formulation is identical to that in [21]. It is assumed that the low frequency plant dynamics can be approximated by a double integrator with an uncertain gain:

$$\tilde{G}(s) = \frac{k_p}{s^2}, \quad 0.1 \leq k_p \leq 10. \quad (4.1)$$

Notice that the ratio of  $k_{p,max}$  to  $k_{p,min}$  is as large as 100. The model is assumed valid up to the frequency  $\omega_o = 100$  rad/s. The parameters  $k_p$  and  $\omega_o$  do not necessarily reflect physical meaningful numbers, however, this is of minor importance here, since the main objective is to illustrate different design techniques. The robust performance control problem is thus to design a fixed dynamic controller which stabilizes the plant and complies with performance demands for all possible plants. To ensure that the controller rolls off at frequencies above  $\omega_o$  a complementary sensitivity specification is included into the design. Performance requirements are given as a standard sensitivity specification. The control problem can then be specified as in Figure 4.1.

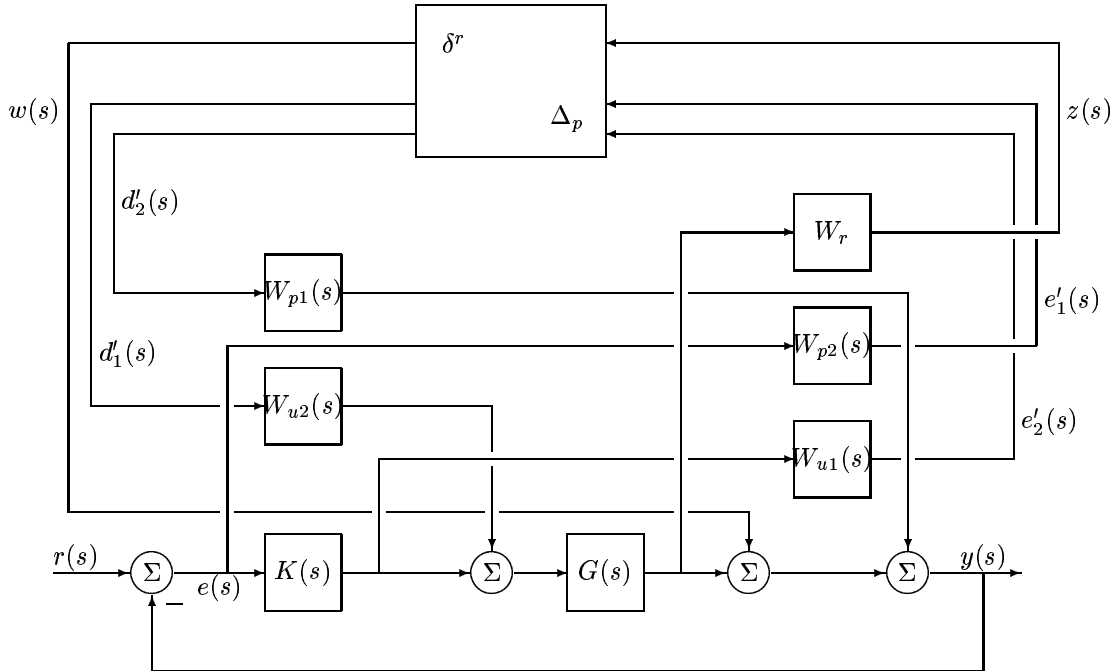


Figure 4.1: Control problem set-up for the C.D. servo drive.

Notice that the perturbed low frequency plant (4.1) can be written

$$\tilde{G}(s) = \frac{1}{s^2} (5.05 + 4.95\delta^r) = \frac{5.05}{s^2} \left( 1 + \frac{4.95}{5.05}\delta^r \right) = G(s) (1 + W_r\delta^r) \quad (4.2)$$

where  $\delta^r \in \mathbf{R}$  is a real scalar perturbation  $\delta^r \in [-1, 1]$ . The sensitivity weights on  $S(s)$  and  $T(s)$  are standard weights taken from [21]:

$$W_{u1}(s) = W_{u2}(s) = \frac{5(s + 0.001)}{s + 5} \quad (4.3)$$

$$W_{p1}(s) = W_{p2}(s) = \frac{0.03}{s + 0.05} \quad (4.4)$$

Notice that we have gathered the weighted sensitivity functions  $W_{p2}SW_{p1}$  and  $W_{u1}TW_{u2}$  into a single performance specification. Our first approach will be to design a complex  $\mu$  optimal controller:

$$K_{\mu_c}(s) = \inf_{K(j\omega) \in \mathcal{K}} \sup_{\omega} \mu_{\tilde{\Delta}_c}(F_l(N(j\omega), K(j\omega))) \quad (4.5)$$

Hence, at first we approximate the real perturbation  $\delta^r$  with a complex one  $\delta^c$ . The complex  $\mu$  problem was solved using  $D$ - $K$  iteration as outlined in Procedure 3.1. The results from the iteration is shown in Figure 4.2 and tabulated in Table 4.1. In Figure 4.2  $\mu_{\tilde{\Delta}_c}(F_l(N(j\omega), K(j\omega)))$  for each iteration is shown across frequency. As seen the iteration converges rapidly with a final complex  $\mu$  peak at 1.41. In Figure 4.2 also the mixed  $\mu$  result for the final controller  $K_{\mu_c}(s)$  is shown. Notice how there is a noticeable dive in mixed  $\mu$  around 0.5 rad/s. It thus seem possible that a significant improvement in control performance can be obtained by applying mixed  $\mu$  synthesis. The results in Figure 4.2 are equivalent to the results presented in [21].

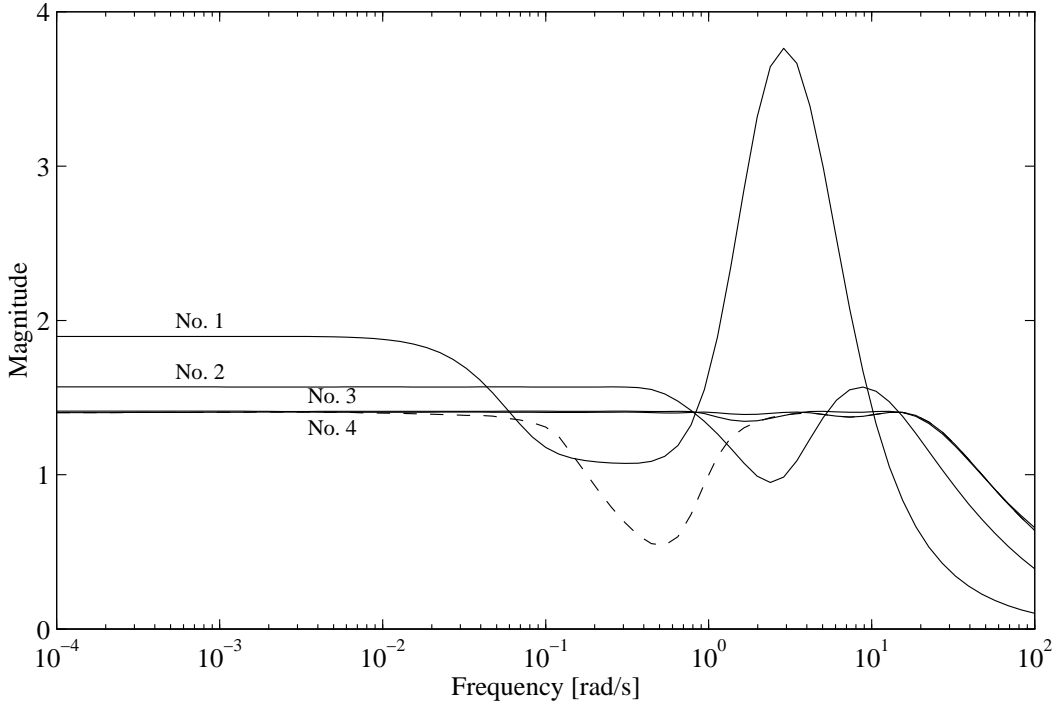


Figure 4.2: Results from  $D$ - $K$  iteration on the  $C.D.$  player servo. Shown are  $\mu_{\tilde{\Delta}_c}(F_l(N(j\omega), K(j\omega)))$  for each iteration and also  $\mu_{\tilde{\Delta}}(F_l(N(j\omega), K(j\omega)))$  for the final complex  $\mu$  controller  $K_{\mu_c}(s)$ .

In order to improve the results from the  $D$ - $K$  iteration,  $\mu$ - $K$  iteration as outlined in Procedure 3.2 was applied to the servo problem. The complex  $\mu$  optimal controller  $K_{\mu_c}(s)$  is then an obvious choice for the initial controller  $K_0(s)$ . In Table 4.1, the results of the  $\mu$ - $K$  iteration is given. Notice how  $\sup_{\omega} \beta(\omega)$  converges to zero indicating that the  $\gamma$  scalings approximates the mixed to complex  $\mu$  ratio. The  $\infty$ -norm  $\|F_l(P_i(s), K_i(s))\|_{\infty}$  is monotonically decreasing as shown in Appendix A. The upper bound  $\bar{\alpha}_i$  were equal to one except for the last 2 iterations. However,  $\kappa$  had to be reduced for each iteration in order to reduce the  $\beta$  peaks (mixed  $\mu$  pop-up phenomena).

In Figure 4.3, mixed and complex  $\mu$  is shown for the initial (complex  $\mu$  optimal) and final mixed  $\mu$  optimal controller. Mixed  $\mu$  peaks at approximately 1.03 and a 25% improvement has thus been obtained through

Iteration No.	$D$ - $K$ Iteration				$\mu$ - $K$ Iteration					
	1	2	3	4	1	2	3	4	5	6
$\ \mu_{\tilde{\Delta}_c}(F_l(N(s), K_i(s)))\ _\infty$	3.76	1.57	1.413	1.406						2.46
$\ \mu_{\tilde{\Delta}}(F_l(N(s), K_i(s)))\ _\infty$				1.406	1.23	1.12	1.11	1.10	1.05	1.03
$\sup_\omega \beta_i(\omega)$				0.61	0.23	0.14	0.13	0.11	0.05	0.03
$\ F_l(P_i(s), K_i(s))\ _\infty$				284	2.48	1.17	1.12	1.05	1.03	1.02
$\inf_\omega \bar{\alpha}_i(\omega)$					1	1	1	1	0.56	0.50
$\kappa$					0.8	0.8	0.8	0.5	0.8	0.8

Table 4.1: Results from  $D$ - $K$  and  $\mu$ - $K$  iteration on the  $C.D.$  player servo.

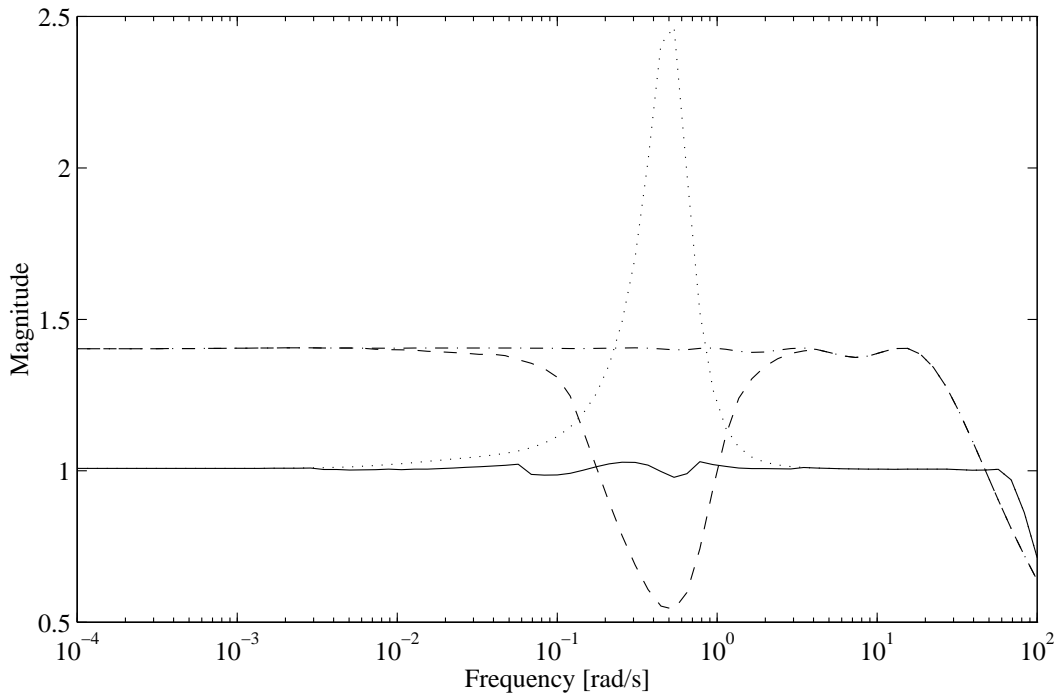


Figure 4.3: Results from  $\mu$ - $K$  iteration on the  $C.D.$  player servo. Shown are  $\mu_{\tilde{\Delta}}(F_l(N(j\omega), K(j\omega)))$  (dashed and solid) and  $\mu_{\tilde{\Delta}_c}(F_l(N(j\omega), K(j\omega)))$  (dash-dotted and dotted) for the initial (complex  $\mu$  optimal) and final mixed  $\mu$  optimal controller respectively.

$\mu$ - $K$  iteration. Notice how this is achieved at the expense of complex  $\mu$ , which peaks at almost 2.5 for the mixed  $\mu$  optimal controller  $K_\mu(s)$ .

In [21],  $G, D$ - $K$  iteration is used to find a mixed  $\mu$  controller for the C.D. player servo. Here mixed  $\mu$  was reported to peak at 1.25 for a ninth order realization of the final mixed  $\mu$  controller. In order to compare this result with the  $\mu$ - $K$  iteration result, the final controller  $K_\mu(s)$ , which had 28 states must be reduced using model reduction. Using the routines provided in the MATLAB  $\mu$  toolbox,  $K_\mu(s)$  was reduced to ninth order with virtually no increase in  $\mu$ . With the reduced order controller  $K_{\mu,r}(s) \mu_{\underline{\Delta}}(F_i(N(j\omega), K_{\mu,r}(j\omega)))$  also peaked at 1.03. For lower order realizations there were a significant increase in mixed  $\mu$ . In this case, it thus seems that  $\mu$ - $K$  iteration performs better than  $G, D$ - $K$  iteration. We believe that the reason for this is problems in fitting the  $G$  scalings. In Figure 4.4, the  $G(\omega)$  is shown for the final mixed  $\mu$  controller  $K_\mu(s)$ . Notice that  $G(\omega)$  is identically zero for a large part of the frequency range (namely at those frequency points where mixed and complex  $\mu$  are identical) but rapidly rise to approximately  $2 \cdot 10^4$  at those frequencies where mixed and complex  $\mu$  differs. Fitting an all-pass transfer function to this kind of data will be very difficult. The corresponding  $\gamma$  scaling in  $\mu$ - $K$  iteration behaves much better as can be seen in Figure 4.4.

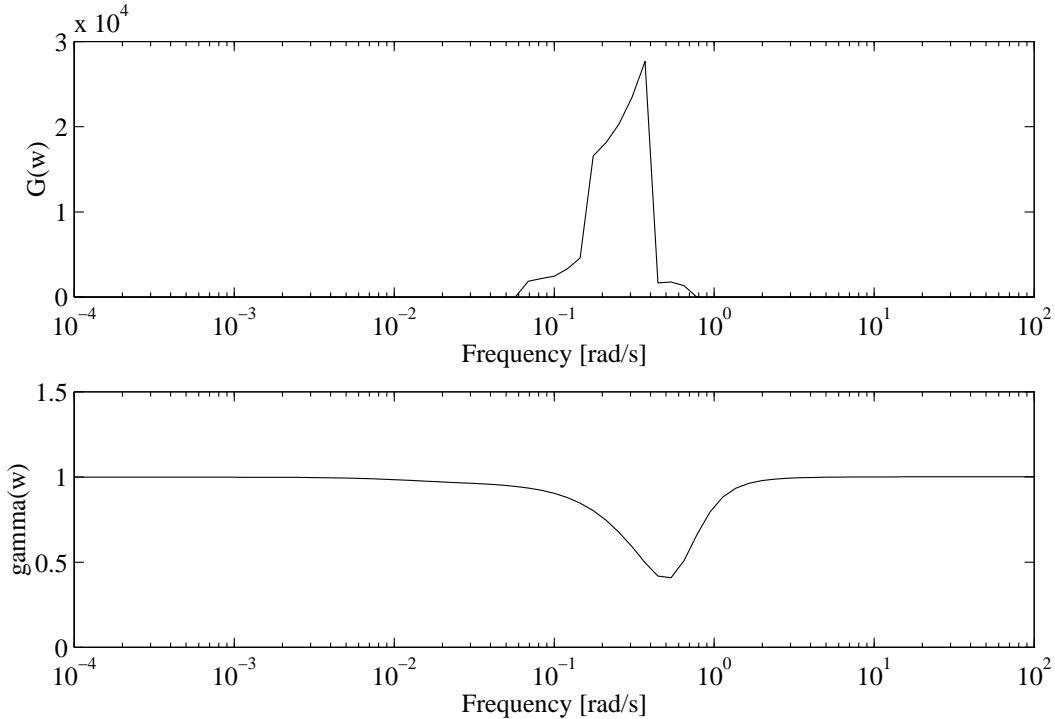


Figure 4.4:  $G$  scalings to be fitted in  $G, D$ - $K$  iteration (top) and  $\gamma$  scalings to be fitted in  $\mu$ - $K$  iteration (bottom).

## 4.2 Water Tank System

In this example level and temperature control of the watertank shown in Figure 4.5 will be considered. In the figure  $m_c$ ,  $T_c$ ,  $m_h$  and  $T_h$  represent massflow and temperature of cold and hot water respectively.  $H$  and  $T$  denote level and temperature in the tank which are the outputs to be controlled. The main disturbance is the massflow  $m_o$  of water tapped from the tank

From first principles the below linearized model of the watertank can be derived using concentrated parameters

$$H(s) = \frac{1}{A\rho s}(m_c(s) + m_h(s) - m_o(s)) \quad (4.6)$$

$$T(s) = \frac{1}{m_{o0}(\tau s + 1)}((T_c - T_{o0})m_c(s) + (T_h - T_{o0})m_h(s)) = G_T(s)(K_c m_c(s) + K_h m_h(s)) \quad (4.7)$$

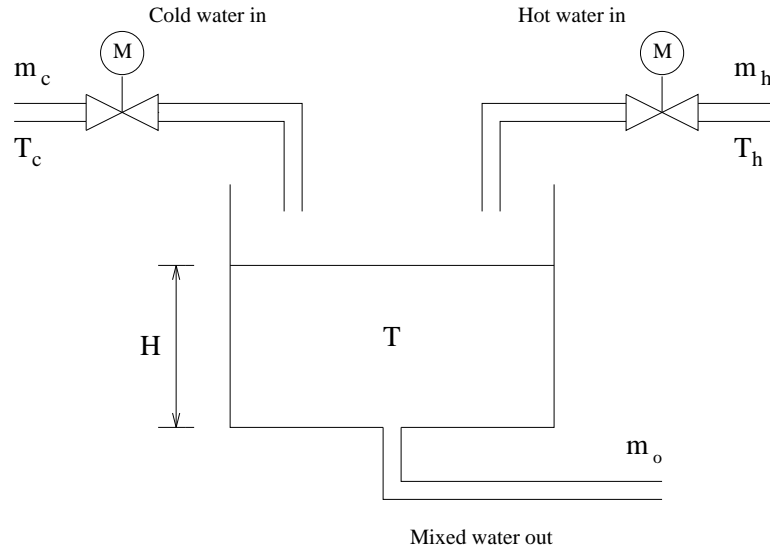


Figure 4.5: *Water tank with cold and hot water supply.*

where  $\rho$  is the density of water,  $A$  is the tank surface area and subscript 0 denote operating point value. The timeconstant of the temperature system is

$$\tau = \frac{\rho AH_0}{m_{o0}} \quad (4.8)$$

The valves have local control loops with a measurement of massflow giving them a unity DC gain. The dynamics of the valves can be described by

$$m_c(s) = \frac{e^{-sT_v}}{s\tau_v + 1} m_{c,ref}(s) = G_v(s) m_{c,ref}(s) \quad (4.9)$$

$$m_h(s) = \frac{e^{-sT_v}}{s\tau_v + 1} m_{h,ref}(s) = G_v(s) m_{h,ref}(s) \quad (4.10)$$

The delays will be approximated by first order Pade functions:

$$e^{-sT_v} \approx \frac{1 - sT_v/2}{1 + sT_v/2} \quad (4.11)$$

The sensors have dynamics which can be approximated as first order systems.

$$H_m(s) = \frac{1}{\tau_H s + 1} H(s) \quad (4.12)$$

$$T_m(s) = \frac{1}{\tau_T s + 1} T(s) \quad (4.13)$$

There are several sources to uncertainty in this model, and only what is believed to be dominating is considered. The uncertainty of the dynamical behavior of the valves is described as multiplicative uncertainty with complex perturbations acting on each valve.

$$G_{vc}(s) = G_v(s)(1 + W_{vc}(s)\Delta_{vc}) \quad (4.14)$$

$$G_{vh}(s) = G_v(s)(1 + W_{vh}(s)\Delta_{vh}) \quad (4.15)$$

$$W_{vc}(s) = W_{vh}(s) = K_w v \frac{s + b_v}{s + a_v} \quad (4.16)$$

Changes in operating point are important sources to uncertainty in Eq. 4.7 and can be separated according to the individual variables forming the operating point.

Changing the operating point for the temperature give reason to changes in gain in  $K_c$  and  $K_h$ , so does also changes in the temperatures of cold and hot supply water. This can conveniently be described by

multiplicative uncertainties with real perturbations.

$$K_{c,pert} = K_c(1 + W_c\Delta_c) \quad (4.17)$$

$$K_{h,pert} = K_h(1 + W_h\Delta_h) \quad (4.18)$$

where  $\Delta_c$  and  $\Delta_h$  are in the interval  $[-1,1]$ .  $G_T(s)$  is affected by changes in the operating points  $m_{o0,pert} = m_{o0}(1 + W_m\Delta_m)$  and  $H_{0,pert} = H_0(1 + W_H\Delta_H)$  giving the change

$$G_{T,pert}(s) = \frac{1}{m_{o0}(1 + W_m\Delta_m)} \frac{1}{1 + s\tau \frac{1 + W_H\Delta_H}{1 + W_m\Delta_m}} \quad (4.19)$$

$$= \frac{1}{m_{o0}(1 + s\tau) \left(1 + \frac{W_m}{1 + s\tau}\Delta_m + \frac{s\tau W_H}{1 + s\tau}\Delta_H\right)} \quad (4.20)$$

As it is shown in Figure 4.6 this perturbation can be described by inverse multiplicative uncertainty with real perturbations corresponding to deviations in operating point. In this construction dynamic weighting functions are used.  $W_H$  and  $W_m$  correspond to the maximum size of perturbations in  $H_o$  and  $m_{o0}$  with  $\Delta_H$  and  $\Delta_m$  being real in the interval  $[-1,1]$ .

$$W_{uH}(s) = \frac{s\tau W_H}{1 + s\tau} \quad (4.21)$$

$$W_{um}(s) = \frac{W_m}{1 + s\tau} \quad (4.22)$$

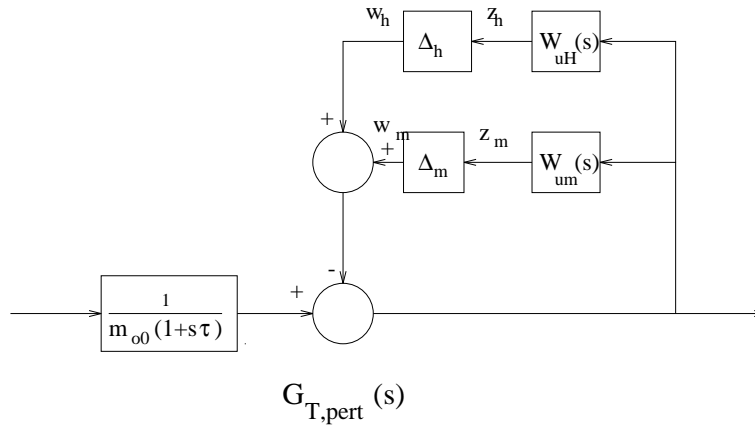


Figure 4.6: *Inverse multiplicative perturbation of  $G_T(s)$ .*

The most important disturbance input to the system is load of tapped water  $m_o$ . Load variations are typically stepwise, and are modelled by a constant  $K_{d1}$ .

$$m_o(s) = K_{d1}d_1'(s) \quad (4.23)$$

where  $\|d_1\|_2 \leq 1$  Another disturbance is noise,  $d_H$ , corrupting the level measurement. This noise is concentrated in the high frequency domain.

$$d_H(s) = \frac{K_{d2}(s + b_{d2})}{s + a_{d2}}d_2'(s) = W_{d2}(s)d_2'(s) \quad (4.24)$$

where  $\|d_2\|_2 \leq 1$ . Changes in setpoint are not important and have been disregarded in the design set-up.

Errors in the outputs H and T should be minimized in the way, that low frequency and DC errors are punished harder than high frequency errors. This will be done forming weighted outputs  $e'$  with lowpass weighting functions.

$$e_1'(s) = K_{p1} \frac{s + b_{p1}}{s + a_{p1}} H(s) = W_{p1}(s)H(s) \quad (4.25)$$

$$e_2'(s) = K_{p2} \frac{s + b_{p2}}{s + a_{p1}} T(s) = W_{p2}(s)T(s) \quad (4.26)$$

This specification can now be put into the  $\mu$  framework see Figure 3.1 with

$$\begin{aligned}
 u &= \begin{bmatrix} m_{c,ref} \\ m_{h,ref} \end{bmatrix} & y &= \begin{bmatrix} H_m \\ T_m \end{bmatrix} & d' &= \begin{bmatrix} d'_1 \\ d'_2 \end{bmatrix} & e' &= \begin{bmatrix} e'_1 \\ e'_2 \end{bmatrix} \\
 w &= \begin{bmatrix} w_{Tc} \\ w_{Th} \\ w_m \\ w_h \\ w_{vc} \\ w_{vh} \end{bmatrix} & z &= \begin{bmatrix} z_{Tc} \\ z_{Th} \\ z_m \\ z_h \\ z_{vc} \\ z_{vh} \end{bmatrix} & \Delta &= \begin{bmatrix} \Delta_{Tc} \\ \Delta_{Th} \\ \Delta_m \\ \Delta_h \\ \Delta_{vc} \\ \Delta_{vh} \end{bmatrix}
 \end{aligned} \tag{4.27}$$

where the elements in  $w$  and  $z$  represent obvious signals in the perturbations described above.

Data used in design is shown in the Table 4.2.

Plant data	A	$\pi * 0.1^2 m^2$	Operating point	$T_c$	$10^\circ C$	
	$\rho$	$1000 kg/m^3$		$T_h$	$60^\circ C$	
	$\tau_H$	$0.3 sec$		$T_{o0}$	$30^\circ C$	
	$\tau_T$	$15.0 ; sec$		$H_0$	$0.4 m$	
	$\tau_v$	$0.15 sec$		$m_{o0}$	$0.3 kg/sec$	
	$T_v$	$0.4 sec$		Disturbance weights	$K_{d1}$	$0.3 kg/sec$
	Uncertainty weights	$W_c$			0.75	$K_{d2}$
$W_h$		0.67	$a_{d2}$		$5.88 sec^{-1}$	
$W_m$		0.67	$b_{d2}$		$0.33 sec^{-1}$	
$W_H$		0.75	Error Weights	$K_{p1}$	$50 m^{-1}$	
$W_v$		2.0		$a_{p1}$	$0.1 sec^{-1}$	
$a_{uv}$		6.7		$b_{p1}$	$1.0 sec^{-1}$	
$b_{uv}$		268		$K_{p2}$	$1.0^\circ C^{-1}$	
		$a_{p2}$		$0.01 sec^{-1}$		
		$b_{p1}$	$0.1 sec^{-1}$			

Table 4.2: Design data for the water tank control problem.

The control problem formulated for the water tank is thus a mixed  $\mu$  problem with two complex and four real scalar uncertainty blocks. The uncertainty structure is augmented with a  $2 \times 2$  full complex performance block. At first the corresponding complex problem was solved using  $D$ - $K$  iteration. Again the iteration converged quickly. After 5 iterations, no significant improvement in  $\mu_{\Delta_c}(F_l(N(j\omega), K_i(j\omega)))$  could be obtained, see Figure 4.7 and Table 4.3. Complex  $\mu$  peaked at 1.30 and robust performance was consequently not obtained. The final complex  $\mu$  controller  $K_{\mu_c}(s)$  was then tested using the true mixed perturbation set. The result is shown in Figure 4.7. Notice that similarly to the servo example there is a decrease in mixed  $\mu$  in the mid frequency area. However, the difference between complex and mixed  $\mu$  is not as large as for the servo controller. Thus in this case the complex perturbation approximation is better and only slight improvement seems possible using mixed  $\mu$  methods like  $G$ ,  $D$ - $K$  or  $\mu$ - $K$  iteration. Nevertheless  $\mu$ - $K$  iteration was applied to the system. The results are given in Table 4.3.

Iteration No.	$D$ - $K$ Iteration				$\mu$ - $K$ Iteration				
	1	2	3	4	1	3	5	7	9
$\ \mu_{\Delta_c}(F_l(N(s), K_i(s)))\ _\infty$	1.93	1.34	1.30	1.30					1.42
$\ \mu_{\Delta}(F_l(N(s), K_i(s)))\ _\infty$				1.30	1.27	1.27	1.24	1.22	1.208
$\sup_\omega \beta_i(\omega)$				0.21	0.19	0.10	0.09	0.073	0.065
$\ F_l(P_i(s), K_i(s))\ _\infty$				1231	1.31	1.24	1.17	1.15	1.14
$\inf_\omega \bar{\alpha}_i(\omega)$					1	1	0.45	0.15	0.006
$\kappa$					0.2	0.5	0.5	0.5	1.0

Table 4.3: Results from  $D$ - $K$  and  $\mu$ - $K$  iteration on the water tank system.

Notice that both  $\sup_\omega \beta_i(\omega)$  and  $\|F_l(P_i(s), K_i(s))\|_\infty$  are monotonically decreasing. The algorithm converges somewhat slower this time. In Figure 4.8 mixed and complex  $\mu$  is shown for the initial (complex  $\mu$  optimal) and final mixed  $\mu$  optimal controller. Here mixed  $\mu$  peaks at approximately 1.20. Consequently

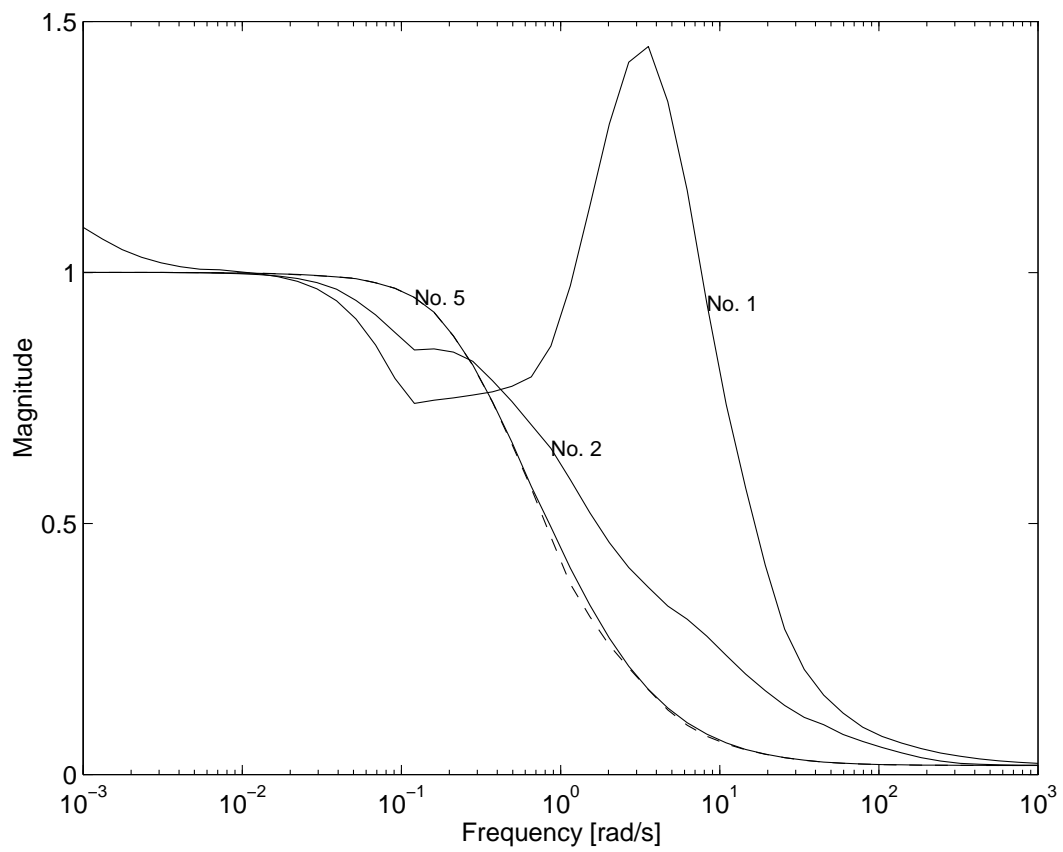


Figure 4.7: Results from D-K iteration on the water tank system. Shown are  $\mu_{\tilde{\Delta}_c}(F_l(N(j\omega), K(j\omega)))$  for iteration 1, 2 and 5 and also  $\mu_{\tilde{\Delta}}(F_l(N(j\omega), K(j\omega)))$  for the final complex  $\mu$  controller  $K_{\mu_c}(s)$ .



the obtained improvement over complex  $\mu$  is rather small. The improvement is obtained at the cost of much higher order of the controller. Whereas the final complex  $\mu$  controller had 51 states, the final mixed  $\mu$  controller had 87 states. Both controllers, however, could be reduced to 25th order with very little degradation in  $\mu$ .

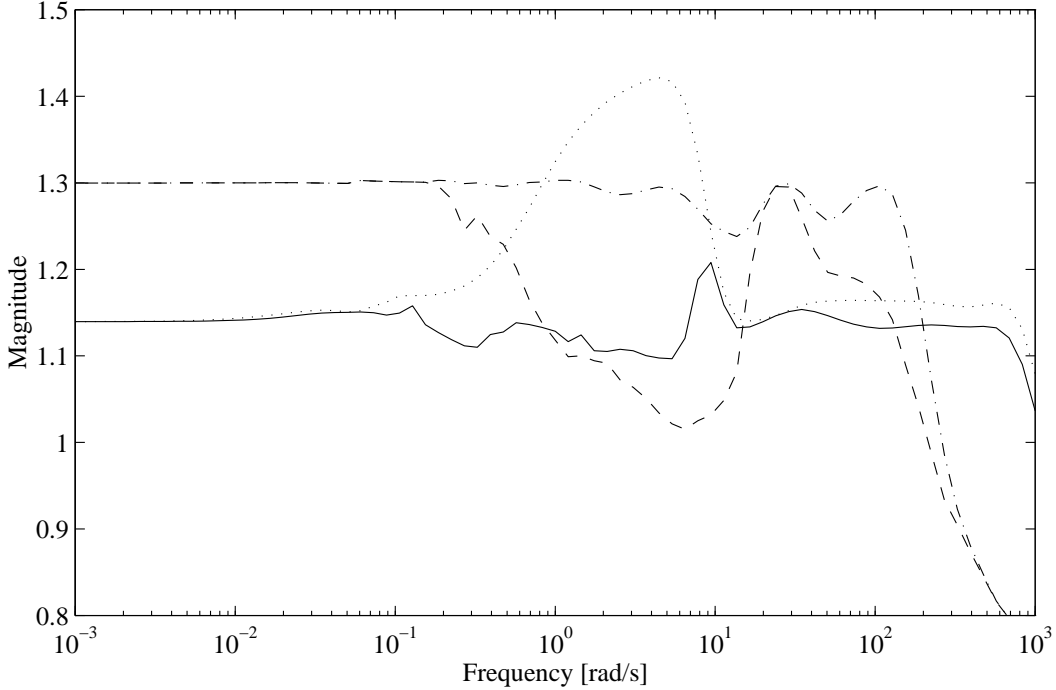


Figure 4.8: Results from  $\mu$ - $K$  iteration on the water tank system. Shown are  $\mu_{\Delta}(F_l(N(j\omega), K(j\omega)))$  (dashed and solid) and  $\mu_{\Delta_e}(F_l(N(j\omega), K(j\omega)))$  (dash-dotted and dotted) for the initial (complex  $\mu$  optimal) and final mixed  $\mu$  optimal controller respectively.

Since robust performance could not be obtained for the given problem, the robust stability and nominal performance conditions will be checked. Recall that

$$\mu_{\Delta}(F_l(N(j\omega), K(j\omega))) \leq 1 \Leftrightarrow \text{robust stability} \quad (4.28)$$

$$\sup_{\omega} \bar{\sigma}(P_{22}(j\omega)) < 1 \Leftrightarrow \text{nominal performance} \quad (4.29)$$

In Figure 4.9 tests for robust stability and nominal performance are shown. It is seen, that the robust stability condition is violated since  $\mu_{\Delta}(F_l(N(j\omega), K(j\omega)))$  peaks at 1.14. The closed loop system will therefore become unstable for the given perturbations and the mixed  $\mu$  controller. Since  $\sup_{\omega} \bar{\sigma}(P_{22}(j\omega))$  nominal performance is achieved.

Thus an alternative design must be made, where e.g. either the performance demands or the range of operating points could be relaxed.

## 5 Conclusion

This paper give an introduction to methods for analysis and synthesis of robust controllers based on  $\mathcal{H}_{\infty}$  and  $\mu$  theory. In chapter 2 a convenient way to specify performance using singular values and the  $\mathcal{H}_{\infty}$  norm is presented along with The Small Gain Theorem which give give a necessary and sufficient condition for robust stability for plants with unstructured perturbations with frequency dependent bounds on singular values.

The  $\mathcal{H}_{\infty}$  optimal controller which is also presented can solve the robust stability problem and the nominal performance problem separately. However it is demonstrated by the use of examples that a non-conservative controller for the robust performance problem will in generally not be obtained as an  $H_{\infty}$

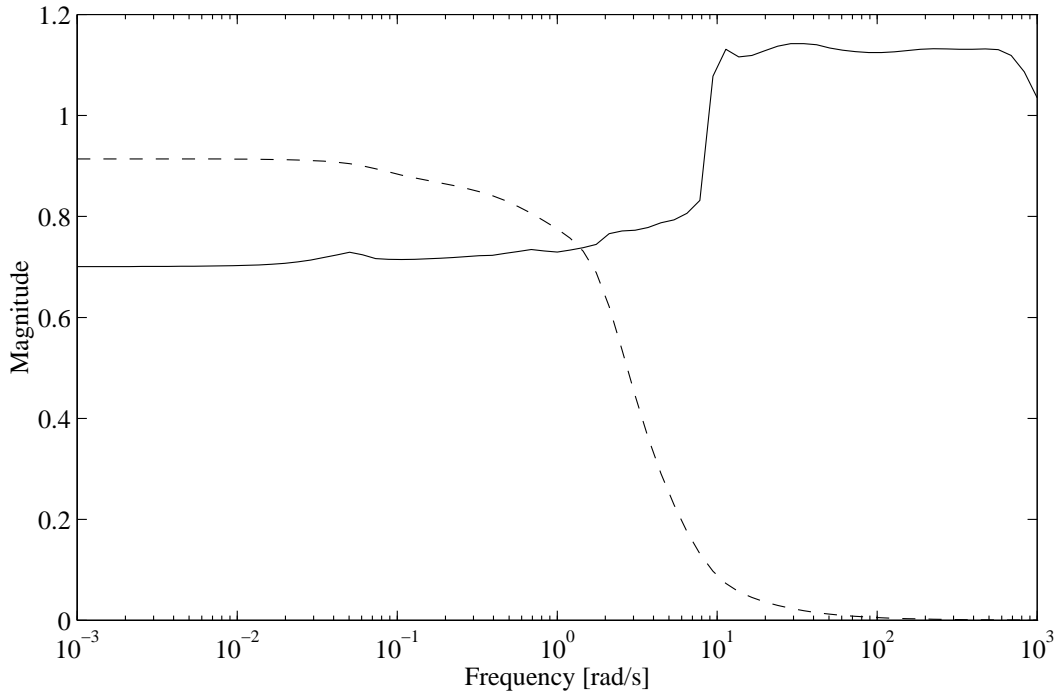


Figure 4.9:  $\mu$  and  $\mathcal{H}_\infty$  conditions for robust stability (solid) and nominal performance (dashed).

optimal controller. For plants with simple output multiplicative or additive uncertainty specification can be conservative by a factor 2, whereas plants with input multiplicative uncertainty can be arbitrarily conservative if they are ill conditioned.

In Section 3 the structured singular value  $\mu$  is presented and is used to formulate tight conditions for robust stability and robust performance for plants with structured or unstructured uncertainty descriptions.

$\mu$  synthesis using  $D$ - $K$  iteration can be effectively used for design of controllers for systems with complex uncertainty blocks. For systems with mixed real and complex uncertainty blocks synthesis with Peter Young's  $G$ , $D$ - $K$  iteration can be used, see [5]. An alternative to this algorithm is the  $\mu$ - $K$  iteration developed by Tøffner-Clausen et al. [7] which seem to have some advantages.

Two design examples are given. A C.D. Player Servo problem is borrowed from Peter Young in order to be able to compare results from the two algorithms for mixed  $\mu$  synthesis. The results show some difference in favor of the  $\mu - K$  algorithm. The other example is a watertank level and temperature is controlled. It is demonstrated how uncertainties coming from changes in operating point can be expressed via uncertainty blocks with real perturbations. For components with partly unmodelled dynamics the uncertainty can be expressed via blocks with complex perturbations. For the water tank example analysis of a controller designed on the basis on only complex perturbations showed that complex and mixed  $\mu$  only differed little meaning that this controller was close to optimal. The subsequent mixed  $\mu$  synthesis gave only marginal improvements.

# Appendices

## A Proof of Lemma 3.1

Here it will be shown that the minimizations:

$$K_i(s) = \inf_{K(s) \text{ stab.}} \sup_{\omega} \{ \bar{\sigma} (F_l (P_{i-1}(j\omega), K(j\omega))) \} \quad (\text{A.1})$$

$$D_i^*(\omega) = \inf_D \bar{\sigma} (D F_l(N(j\omega), K_i(j\omega)) D^{-1}), \quad \forall \omega \quad (\text{A.2})$$

are monotonically non-increasing in  $\|F_l(P_i, K_i)\|_{\infty}$ . Given a controller  $K_i(s)$  and scaling matrices  $\Gamma_i(s)$  and  $D_i(s)$  it is clear from (3.39) that:

$$\|F_l(P_i(s), K_i(s))\|_{\infty} = \sup_{\omega} |\gamma_i(j\omega)| \bar{\sigma} (F_l (D_i(j\omega)N(j\omega)D_i^{-1}(j\omega), K_i(j\omega))) \quad (\text{A.3})$$

Furthermore, assuming perfect realizations of the  $\gamma_i(s)$  scalings, we have that

$$|\gamma_i(j\omega)| = (1 - \alpha_i) |\gamma_{i-1}(j\omega)| + \alpha_i \frac{\bar{\mu}_{\bar{\Delta}} (F_l (N(j\omega), K_i(j\omega)))}{\bar{\mu}_{\bar{\Delta}_c} (F_l (N(j\omega), K_i(j\omega)))} \quad (\text{A.4})$$

$$= |\gamma_{i-1}(j\omega)| \left( 1 + \alpha_i \left( \frac{\bar{\mu}_{\bar{\Delta}} (F_l (N(j\omega), K_i(j\omega)))}{\bar{\mu}_{\bar{\Delta}_c} (F_l (N(j\omega), K_i(j\omega)))} \frac{1}{|\gamma_{i-1}(j\omega)|} - 1 \right) \right) \quad (\text{A.5})$$

$$= |\gamma_{i-1}(j\omega)| (1 + \alpha_i \beta_i(\omega)) \quad (\text{A.6})$$

Consequently:

$$\|F_l(P_i(s), K_i(s))\|_{\infty} = \sup_{\omega} (1 + \alpha_i \beta_i(\omega)) |\gamma_{i-1}(j\omega)| \bar{\sigma} (F_l (D_i(j\omega)N(j\omega)D_i^{-1}(j\omega), K_i(j\omega))) \quad (\text{A.7})$$

In order to achieve a monotonically non-increasing algorithm it is thus required that

$$\sup_{\omega} (1 + \alpha_i \beta_i(\omega)) |\gamma_{i-1}(j\omega)| \bar{\sigma} (F_l (D_i(j\omega)N(j\omega)D_i^{-1}(j\omega), K_i(j\omega))) \leq \|F_l(P_{i-1}(s), K_{i-1}(s))\|_{\infty} \quad (\text{A.8})$$

We now have the inequalities

$$|\gamma_{i-1}(j\omega)| \bar{\sigma} (F_l (D_i(j\omega)N(j\omega)D_i^{-1}(j\omega), K_i(j\omega))) \leq |\gamma_{i-1}(j\omega)| \bar{\sigma} (F_l (D_{i-1}(j\omega)N(j\omega)D_{i-1}^{-1}(j\omega), K_i(j\omega))) \quad (\text{A.9})$$

$$\leq \sup_{\omega} |\gamma_{i-1}(j\omega)| \bar{\sigma} (F_l (D_{i-1}(j\omega)N(j\omega)D_{i-1}^{-1}(j\omega), K_i(j\omega))) \quad (\text{A.10})$$

$$\leq \sup_{\omega} |\gamma_{i-1}(j\omega)| \bar{\sigma} (F_l (D_{i-1}(j\omega)N(j\omega)D_{i-1}^{-1}(j\omega), K_{i-1}(j\omega))) \quad (\text{A.11})$$

$$= \|F_l(P_{i-1}(s), K_{i-1}(s))\|_{\infty} \quad (\text{A.12})$$

The first inequality follows from (A.2) with perfect realizations of the scalings  $D_i(s)$ . The last inequality follows from (A.1). Since  $\alpha_i \in [0; 1]$  and  $\beta_i(\omega) \geq -1$  it then becomes clear from (A.9-A.12) and (A.7) that if  $\beta_i(\omega) \leq 0, \forall \omega \geq 0$  then

$$\|F_l(P_i(s), K_i(s))\|_{\infty} \leq \|F_l(P_{i-1}(s), K_{i-1}(s))\|_{\infty}, \quad \text{for } \sup_{\omega} \beta_i(\omega) \leq 0 \quad (\text{A.13})$$

and the algorithm will be monotonically non-increasing for all values of  $\alpha_i$ . We may hence choose  $\alpha_i = 1$ . If  $\beta_i(\omega) < 0, \forall \omega \geq 0$  it is thus guaranteed that the  $\infty$ -norm  $\|F_l(P_i(s), K_i(s))\|_{\infty}$  will be reduced during the  $i$ th step of the iteration.

If  $\beta_i(\omega) > 0$  for any frequency  $\omega$  we must choose  $\alpha$  so that (A.8) is fulfilled. Since the frequency at which the supremum is reached depends on  $\alpha_i$  we must solve the inequality for all frequencies  $\omega$ . Let  $\bar{\alpha}_i$  denote the solution to (A.8) with inequality replaced with equality. It is easily verified that

$$\bar{\alpha}_i(\omega) = \left( \frac{\|F_l(P_{i-1}(s), K_{i-1}(s))\|_{\infty}}{\bar{\sigma} (F_l (D_i(j\omega)N(j\omega)D_i^{-1}(j\omega), K_i(j\omega))) |\gamma_{i-1}(j\omega)|} - 1 \right) \frac{1}{\beta_i(\omega)} \quad (\text{A.14})$$

Thus if we choose  $\alpha_i$  such that  $\alpha_i \leq \min_{\omega} \bar{\alpha}_i(\omega)$  then (A.8) will be fulfilled and the algorithm will be monotonically non-increasing if  $\alpha_i \geq 0$ . From (A.9) we have that

$$\|F_l(P_{i-1}(s), K_{i-1}(s))\|_{\infty} \geq \bar{\sigma}(F_l(D_i(j\omega)N(j\omega)D_i^{-1}(j\omega), K_i(j\omega))) |\gamma_{i-1}(j\omega)| \quad (\text{A.15})$$

where the equality holds only if  $D_i(j\omega) = D_{i-1}(j\omega)$  and  $K_i(j\omega) = K_{i-1}(j\omega)$  at the particular frequency at which the supremum is reached. Since  $\beta_i(\omega) > 0$  it is then clear from (A.14) and (A.15) that  $\alpha \geq 0$ . If  $\min_{\omega} \bar{\alpha}_i(\omega) > 0$  we may choose  $\alpha_i > 0$  and it will be guaranteed that the  $\infty$ -norm  $\|F_l(P_i(s), K_i(s))\|_{\infty}$  is reduced during the  $i$ th step of the iteration.  $\square$

## References

- [1] S. Tøffner-Clausen, P. Andersen, J. Stoustrup, and Hans Henrik Niemann. Estimated frequency domain model uncertainties used in robust controller design — a  $\mu$ -approach. In *Proc. 3rd IEEE Conf. on Control Applications*, volume 3, pages 1585–1590, Glasgow, Scotland, Aug. 1994.
- [2] G.J. Balas, J.C. Doyle, K. Glover, A. Packard, and R. Smith.  *$\mu$ -Analysis and Synthesis Toolbox*. The MathWorks Inc., Natick, Mass., USA, 2nd edition, July 1993.
- [3] A.M. Holohan. A tutorial on mu-analysis. In *EURACO Network: Robust and Adaptive Control Tutorial Workshop*, University of Dublin, Trinity College, 1994. Lecture 2.5.
- [4] J.C. Doyle and C.-C. Chu. Matrix interpolation and  $\mathcal{H}_{\infty}$  performance bounds. In *Proc. American Control Conf.*, 1985.
- [5] P.M. Young. *Robustness with Parametric and Dynamic Uncertainty*. PhD thesis, California Institute of Technology, Pasadena, California, May 1993.
- [6] P.M. Young. Controller design with mixed uncertainties. In *Proc. American Control Conf.*, pages 2333–2337, Baltimore, Maryland, June 1994.
- [7] S. Tøffner-Clausen, P. Andersen, J. Stoustrup, and H.H. Niemann. A new approach to  $\mu$ -synthesis for mixed perturbation sets. In *Proc. 3rd European Control Conf.*, Rome, Italy, 1995.
- [8] M. Morari and E. Zafriou. *Robust Process Control*. Prentice-Hall Inc., 1989.
- [9] B. Bernhardsson. The  $\mathcal{H}_{\infty}$  approach. In *EURACO Network: Robust and Adaptive Control Tutorial Workshop*, University of Dublin, Trinity College, 1994. Lecture 2.2.
- [10] C.A. Desoer and M. Vidyasagar. *Feedback Systems: Input-Output Properties*. Academic Press, New York, 1975.
- [11] J.C. Doyle and G. Stein. Multivariable feedback design: Concepts for a classical/modern synthesis. *IEEE Trans. Aut. Contr.*, AC-26(1):4–16, February 1981.
- [12] N.A. Lethomaki. *Practical Robustness Measures in Multivariable Control System Analysis*. PhD thesis, Dept. of Electrical Eng. and Computer Science, Massachusetts Institute of Technology, Cambridge, MA, 1981.
- [13] B.A. Francis. *A Course in  $\mathcal{H}_{\infty}$  Control Theory*, volume 88 of *Lecture Notes in Control and Information Sciences*. Springer Verlag, Berlin, 1987.
- [14] J.C. Doyle, K. Glover, P.P. Khargonekar, and B.A. Francis. State space solutions to standard  $\mathcal{H}_2$  and  $\mathcal{H}_{\infty}$  control problems. *IEEE Trans. Aut. Contr.*, AC-34(8):831–847, 1989.
- [15] R.Y. Chiang and M.G. Safonov. *Robust Control Toolbox*. The MathWorks Inc., Natick, Mass., USA, Aug. 1992.
- [16] J.C. Doyle and A. Packard. Uncertain multivariable systems from a state space perspective. In *Proc. American Control Conf.*, pages 2147–2152, Minneapolis, MN, 1987.
- [17] A. Packard and J.C. Doyle. The complex structured singular value. *Automatica*, 29(1):71–109, 1993.
- [18] M.K.H. Fan, A.L. Tits, and J.C. Doyle. Robustness in the presence of mixed parametric uncertainty and unmodeled dynamics. *IEEE Trans. Aut. Contr.*, 36(1):25–38, Jan. 1991.

- [19] P.M. Young, M.P. Newlin, and J.C. Doyle.  $\mu$  analysis with real parametric uncertainty. In *Proc. 30th IEEE Conf. on Decision and Control*, pages 1251–1256, Brighton, England, Dec. 1991.
- [20] J.C. Doyle. Structured uncertainty in control system design. In *Proc. 24th Conf. on Decision and Control*, pages 260–265, 1985.
- [21] P.M. Young and K.J. Åström.  $\mu$  meets bode. In *Proc. American Control Conf.*, pages 1223–1227, Baltimore, Maryland, June 1994.